OECONOMIA
COPERNICANA

VOLUME 13 ISSUE 3 SEPTEMBER 2022

p-ISSN 2083-1277, e-ISSN 2353-1827
www.oeconomia.pl

ORIGINAL ARTICLE

Citation: Boateng, E., Asafo-Adjei, E., Gatsi, J. G., Gherghina, S. C. & Simionescu, L. N. (2022). Multifrequency-based non-linear approach to analyzing implied volatility transmission across global financial markets. *Oeconomia Copernicana, 13*(3), 699–743. doi: 10.24136/oc.2022.021

Contact to corresponding author: Ştefan Cristian Gherghina, stefan.gherghina@fin.ase.ro

Article history: Received: 10.06.2022; Accepted: 27.08.2022; Published online: 25.09.2022

Ebenezer Boateng
University of Cape Coast, Ghana
orcid.org/0000-0001-7297-7943

Emmanuel Asafo-Adjei
University of Cape Coast, Ghana
orcid.org/0000-0002-4449-6285

John Gartchie Gatsi
University of Cape Coast, Ghana
orcid.org/0000-0003-0650-697X

Ştefan Cristian Gherghina
Bucharest University of Economic Studies, Romania
orcid.org/0000-0003-2911-6480

Liliana Nicoleta Simionescu
Bucharest University of Economic Studies, Romania
orcid.org/0000-0001-5494-5673

Multifrequency-based non-linear approach to analyzing implied volatility transmission across global financial markets

JEL Classification: *C6; C58; G11; G14; G01; Q40*

Keywords: *shocks transmission; information flow; Rényi transfer entropy; multi-scale; market conditions*

Abstract

Research background: The contagious impact of the COVID-19 pandemic has heightened financial market's volatility, nonlinearity, asymmetric and nonstationary dynamics. Hence, the existing relationship among financial assets may have been altered. Moreover, the level of investor risk aversion and market opportunities could also alter in the pandemic. Predictably, investors in the heat of the moment are concerned about minimizing losses. In order to determine the level of hedge risks between implied volatilities in the COVID-19 pandemic through information flow, it is required to take into account the increased vagueness of economic projections as well as the increased uncertainty in asset values as a result of the pandemic.
Purpose of the article: The study aims to examine the transmission of information between the VIX-implied volatility index for S&P 500 and fifteen other implied volatility indices in the COVID-19 pandemic.
Methods: We relied on daily changes in the VIX and fifteen other implied volatility indices from commodities, currencies, and stocks. The study employed the improved complete ensemble empirical mode decomposition with adaptive noise which is in line with the heterogeneous expectations of market participants to denoise the data and extract intrinsic mode functions (IMFs). Subsequently, we clustered the IMFs based on common features into high, low, and medium frequencies. The analysis was carried out using Rényi transfer entropy (RTE), which allowed for the evaluation of both linear and non-linear, as well as varied distributions of the market dynamics.
Findings & value added: Findings from the RTE revealed a bi-directional flow of negative information amid the VIX and each of the volatility indices, particularly in the long term. We found this behavior of the markets to be consistent at varying levels of investors' risk aversion. The findings help investors with their portfolio strategies in the time of the pandemic, which has resulted in fluctuating levels of risk aversion. Our findings characterize global financial markets to be "non-linear heterogeneous evolutionary systems". The results also lend support to the emerging delayed volatility of market competitiveness and external shocks hypothesis.

Introduction

The adaptive market hypothesis has brought to light the time-varying dynamics in both market and investor behaviors. Lo (2004) asserts that investment strategies undergo cycles of profit and loss as markets evolve due to their varying degrees of efficiency. As the business environment changes, the size of market participants also alters and profit opportunities vary. The level of market efficiency is thus consequent on how adaptive, innovative, and competitive the market and market participants are (Lekhal & El Oubani, 2020; Owusu Junior *et al*., 2021a). This implies that the risk and reward preferences of market participants may not be universally constant, but can be shaped by the experiences of the market participants themselves. Further, it presupposes that the willingness of investors to innovate is key to their survival in financial markets (Bulathsinhalage & Pathirawasam, 2017).

Innovations in investment strategies are arguably more important now because investment opportunities that were probably apparent in the past three decades may no longer exist. For instance, improvements in crossborder trade and investment flows among countries have resulted in high levels of economic and financial integration. Most emerging and developing economies have institutionalized market-oriented policies (Khoury *et al.*, 2015), encouraging investments from developed economies. While these occurrences have enhanced global financial market development with positive repercussions on access to funding (see, Bui & Bui, 2020; Lim & Kim, 2011; Law & Habibullah, 2009; Le *et al*., 2016), the correlations between various international financial markets might have likewise significantly increased. As a result, the benefits of asset diversification that were previously visible have decreased significantly (Badshah, 2018).

In fact, an understanding of the interrelationships between the assets held in a portfolio is essential to modern portfolio theory. Their interdependencies could alter, which would probably change the riskiness of the portfolio. Since asset correlations may alter in times of crisis, portfolio diversification strategies may not be effective in such periods (see, Gallegati, 2012; Valaskova *et al*., 2021; Barson *et al*., 2022). This could be more severe in the COVID-19 pandemic, which has possibly exacerbated financial risks due to increasing investor uncertainty and shocks to the international flow of funds (Gunay, 2020). Consequently, a preponderance of investment literature from 2020 has arguably been devoted to searching safe-haven assets for equity investors.

Predictably, investors could be more concerned about minimizing losses. A characteristic of investors as advanced by the competitive market hypothesis (CMH) of Owusu Junior *et al.* (2021b) is their updated conflicting risk and reward preferences that force a recalibration of portfolios to fit their shifting risk appetites. This is because economic forecasts are now vaguer and asset prices are more uncertain as a result of the pandemic. Investors switch between markets and combine different instruments as a result of this and anxiety.

Recently, financial markets have witnessed a proliferation of several volatility indices. Given that the Chicago Board Options Exchange (CBOE) Volatility Index (VIX), the widely used investor fear gauge, has a superior informational content (see, Dimpfl & Peter, 2013; Chen & Huang, 2014; Balcilar & Demirer, 2015), it is unclear whether futures on these indexes offer genuine opportunities to hedge risks during the COVID-19 pandemic or if they are essentially a highly correlated, information-overloading of the VIX. The purpose of the current study is to investigate this phenomenon by examining the information flows between the VIX and fifteen volatility indices. We have assembled implied volatility indices comprising: CBOE Euro Currency Volatility; CBOE Gold Volatility; CBOE NASDAQ 100 Volatility; CBOE Crude Oil Volatility; CBOE Russell 2000 Volatility;

DAX New Volatility; DJIA Volatility; Dorsey Wright Developed Market Momentum and Low Volatility; HSI Volatility; CAC 40 VIX; STOXX 50 Volatility VSTOXX; CBOE Vix Volatility_VVIX; CBOE Emerging Markets Etf Volitlity; CBOE Energy Sector Etf Volitlity; and CBOE OEX Implied Volatility.

We use volatility indices rather than prices or returns series of domestic or foreign assets because volatility transmissions clearly and quickly capture the dynamics of market integration (see Peng & Ng, 2012). Moreover, we employ implied volatility indices rather than realized volatility because the latter, which are extracted from price series, are historical in nature (Dutta *et al*., 2017). Implied volatility measures uncertainty accurately since they simultaneously incorporate past price data and investor predictions for future price movements (Badshah *et al*., 2018; Boateng *et al*., 2021). Implied volatility indices are also traded securities and hence can be used for asset allocation and portfolio optimization.

Nevertheless, the variability in implied volatility series is more intense than price series. Volatility indices also depict the asymmetric, abnormal, and time-variant investor behavior (Badshah *et al*., 2018). This presents issues of non-linearities and non-stationarities (Owusu Junior *et al*., 2021b). Additionally, noise — a characteristic feature of financial market data — is usually associated with volatility indices. To deal with such inherent complexities in the dataset, we employ two main strategies. First, we apply the improved complete ensemble empirical mode decomposition with adaptive noise (ICEEMDAN) to denoise the data. Second, we employ the Rényi Transfer Entropy (RTE) to assess the information flows between the VIX and the fifteen implied volatility indices. The latter enables the study to model financial time-series data with characteristics of non-linearities. RTE assigns weights to the distribution and therefore distinguishes between tails of the distribution which addresses tail dependence in the markets (see, Bossman *et al*., 2022a; Bossman, 2021; Asafo-Adjei *et al*., 2021c). Undeniably, existing evidence divulges that volatility indices are tail-distributed (see, Badshah *et al*., 2018; Badshah, 2018). Fat tails can be more noticeable in the pandemic since there would have likely been significant increase in investor risk aversion as a result of the shock and uncertainty.

Several studies have examined the interdependencies among global financial markets. However, studies that examine implied volatility linkages among global financial markets are rare. An attempt by Del Castillo Olivares *et al.* (2018) that investigates implied volatility linkages with twenty-nine volatility indices ignores asymmetric relationships between financial markets. Furthermore, it has been well established in the literature that noise in time series can sometimes be more evident than the effect of the signal, thereby confounding the outcomes (see, Dimpfl & Peter 2014). By denoising the dataset, the study is the first to use a noise-assisted technique to assess implied volatility transmissions across international financial markets. The ICEEMDAN decomposition ensures that the results can also be presented in accordance with the heterogeneous and adaptive nature of financial markets and its participants. Second, applying Rényi transfer entropy to the subject of market diversification offers a non-parametric, nonlinear, and asymmetric lens to the discourse. Since RTE is a form of causality (Owusu Junior *et al.*, 2021b), the findings succor's investors to hedge risk by employing negative pairs in their portfolios.

In the next section, we present a brief literature review. Subsequently, the methodology employed in the study is discussed. Afterwards, the results are disclosed and discussed. Finally, we conclude the study by highlighting practical, theoretical and policy implications.

Literature review

As explained earlier, the justification for examining the relationships among markets with time-varying methodologies is amplified by the adaptive market and heterogeneous market hypotheses. The postulates of Lo (2004) imply that financial markets and profit opportunities in financial markets evolve. Due to shifting market conditions, adaptation, innovation, competition, and mutation cause a decline and a rise in the intensity of market efficiency. Further, Müller *et al.* (1993) explained that financial market participants also have heterogenous expectations which influence the construction of their portfolios.

However, empirical discussions on VIX transmissions to other financial markets have been explored with less attention to information flows and the time-varying nature of markets. Sarwar (2019) investigated risk transmissions between VIX and other volatility indices in emerging markets with VARMAX-DCC-QGARCH model and found that VIX shocks contribute to a large percentage of the prediction error of emerging markets' volatility shocks, but the reverse does not hold.

Similarly, Smales (2022) employed daily changes in G7 and BRIC implied volatility indices over twenty years and documented that the VIX plays a significant role in spreading fear across markets but changes in the uncertainties in the global financial markets do not explain variations in the U.S. market, accentuating the dominance of the U.S market in risk transmissions. Cheuathonghua *et al.* (2019) analyzed VIX transmissions on activities of forty-two international markets during bearish market conditions.

Their study found that VIX exhibit a stronger impact on returns in developed markets and accounts for a larger variation of volatility in emerging markets. Tissaoui and Zaghdoudi (2021) also examined the dynamic connectedness between the VIX and implied volatility indices from Euro-Asian financial markets. Findings from the least square regression using the OLS and spatial model showed that the VIX performs better than domestic risks in explaining fear in European financial markets. This is not the case, though, for Asian markets, where fluctuations in implied volatility indices are caused more by realized volatility than by the VIX.

The empirical discussion of Del Castillo Olivares *et al.* (2018) is closely related to our investigation. Using daily data from March 16, 2011, to May 27, 2015, they investigated the relationships among 29 volatility indexes from markets for commodities, equities, currencies, and fixed income securities. They employed Pearson correlation, Spearman rank correlation, Kendall's tau, principal component analysis, and independent component analysis and documented that the VIX, a market-driven volatility element, predominates in the connections. We build on this study by employing the ICEEMDAN-based RTE to assess the information flows between the markets.

Due to the superiority of the RTE and the importance of decomposing financial time-series data, a nascent body of literature has explored similar techniques to examine the linkages among financial markets albeit they have not considered the nature of information flows between the VIX and other implied volatility indices. In the COVID-19 pandemic, for instance, Bossman *et al.* (2022a) used the ICEEMDAN-based transfer entropy to study the information flows between conventional and Islamic bonds and discovered that there are time-varying investing possibilities between these two types of bonds. By using the ICEEMDAN-induced transfer entropy to analyze the information flows from the COVID-19 pandemic to conventional and Islamic stocks, Bossman (2021) determined that these markets offer diversification opportunities at various time frames.

Similarly, Asafo-Adjei *et al.* (2022c) employed the CEEMDAN-induced RTE and found that a bi-directional causality of information flow between global commodities and uncertainty indices exists in the long term. Further, the time-varying dynamics of the financial markets were amplified as they reported that investors who delayed investment in these markets during the pandemic were likely to minimize risks. Boateng *et al.* (2022b) also employed the CEEMDAN-based RTE framework to quantiify information flows among developed and emerging equity markets. In their findings, they found a mixture of bi-directional and uni-directional flow of both high- and low-risk information. More importantly, they also documented that profit opportunities among the emerging equities varied based on investors' time horizons. However, little is known about information flows among implied volatilities for global financial markets.

Research methods

Data sources and description

The study employs 16 daily implied volatility indices as shown in Table 1. They include volatilities from different forms of financial assets, such as currency, commodities, and conventional equities, in national, regional, or global indexes. After removing the missing data, the daily data spans from 30th January 2020 to 18th August 2021 yielding 1043 observations. The recommended time frame is to reveal the dynamics of information flows among volatility indices during the COVID-19 pandemic, which has distorted the dynamics of most financial markets.

This is particularly important in times of crisis as correlations among assets may break down to induce portfolio diversification strategies, but in cases of increased correlations in longer periods precipitating the low impact of the crises, it opens the floodgates for financial contagion, due to lessened investor uncertainty and shocks to the transnational flow of funds (Gunay, 2020). Conversely, the delayed impact of the pandemic on the dynamics of the volatility indices may distort correlations among the indices in the long term to prompt either diversification or safe-haven benefits. Insights from the dynamics of information flow among the volatility indices in the pandemic would determine the extent to which investors can seek safe haven from other forms of conventional equities or hedge against significant transmitters of shocks in times of crisis. The data used in support of this study was gleaned from investing.com database. The data was executed on daily returns as

$$lnr_t = \ln P_t - lnP_{t-1} \tag{11}$$

where lnr_t denotes the natural logarithmic returns, P_t and P_{t-1} are current and previous volatility indices respectively.

Improved Complete Ensemble Empirical Mode Decomposition with Adaptive Noise (I-CEEMDAN)

According to Ramsey and Lampart (1998), economists albeit not having the tools then have long understood the relationship among finance and economic to alter in degree and direction over time. The ability to decompose financial time series and economic variables into all orthogonal time-scale components have only be plausible in recent times. In addition, there are tools which are now available to deal with the noise that frequently characterizes short-term financial asset series. A noteworthy example is the Improved Complete Ensemble Empirical Mode Decomposition with Adaptive Noise (I-CEEMDAN) which happens to be the most advanced for of Empirical Mode Decompositions (EMDs) of Huang *et al.* (1998). The EMD family have been argued to be superior due to their accuracy in reconstruction, effectiveness, reduced noise-to-signal ratio (SNR) in unsteady-state signals (Huang *et al.*, 1998; Colominas *et al.*, 2014). Colominas *et al.* (2014) notes that ICEEMDAN possesses the best of these qualities as far as decomposition is concerned. However, it falls short counts of contained residue noise which remains in the model and issue of spurious mode (Li *et al.*, 2020).

This study adapts the summary of the ICEEMDAN from Li *et al.* (2020) as follows:

1. a white-noise $\tau_1[\omega^{(i)}]$ is appended to a signal x, which generates a new series

$$x^{(i)} = x + \rho_0\left(\omega^{(i)}\right), i = 1, 2, \ldots, N, \tag{1}$$

where $\omega^{(i)}$, ρ_0, and N represents the i-th added white noise, SNR, and several white noise appended. x represents changes in the implied volatility indices.

2. local mean of $x^{(i)}$ is computed using EMD and the first residual is retrieved as specified below:

$$r_1 = \left(\frac{1}{N}\right) \sum_{i=1}^{N} M\left(x^{(i)}\right), \tag{2}$$

Based on this, first IMF $c_1 = x - r_1$ can be obtained.

3. Through a recursive process, obtain the k-th IMF $c_k = r_{k-1} - r_k$, for $k \geq 2$, where

$$r_k = \left(\frac{1}{N}\right) \sum_{i=1}^{N} M\left(r_{k-1} + \rho_{k-1}\tau_k\left(\omega^{(i)}\right)\right) \quad (3)$$

Interested readers can find further information on the EMD family from Wu and Huang (2009), Flandrin *et al.* (2004), Torres *et al.* (2011), and Li *et al.* (2020).

Rényi transfer entropy

Before addressing the highlights of the Rényi transfer entropy (RTE), it is essential to understand Shannon entropy. This is because RTE explains the level of uncertainty on which transfer entropy (TE) is based (Behrendt et al., 2019; Adam, 2020).We study a probability distribution p_j. From Hartley (1928), the mean information on of every symbol is provided as

$$H = \sum_{j=1}^{n} P_j log_2\left(\frac{1}{P_j}\right) \text{ bits,} \quad (4)$$

where the number of diverse symbols regarding the probabilities P_j is represented by n.

The Shannon entropy (SE) (Shannon, 1948) provides for a discrete random variable (J) with probability distribution ($P(j)$), the mean number of bits desirable for encoding independent draws at the maximum (Behrendt *et al.*, 2019) can be presented as

$$H_J = -\sum_{j=1}^{n} P(j) log_2 P(j) \quad (5)$$

SE employs the notion of Kullback-Leibler distance (Kullback & Leibler, 1951) to quantify the information flows between two-time series variables within the Markov framework. For two discrete random variables, I and J, the marginal probabilities of $P(i)$ and $P(j)$ and joint probability $P(i,j)$, with dynamic structures that resemble a stationary Markov process of order k (Process I) and I (process J). According to the Markov property, the likelihood of seeing I at time $t+1$ in state i consequent on the k prior observations is $p(i_{t+1}|i_t, \dots, i_{t-k+1}) = p(i_{t+1}|i_t, \dots, i_{t-k})$. To encode $t+1$, Given that the ex-ante k observations are known, the average number of bits required may be expressed as follows:

$$h_j(k) = -\sum_i P(i_{t+1}, i_t^{(k)}) log P\left(i_{t+1} \middle| i_t^{(k)}\right) \tag{6}$$

where $i_t^{(k)} = (i_t, \dots, i_{t-k+1})$ (compatibly for process *J*). The information flow from process J to process I under the Kullback-Leibler distance phenomenon in the setting of two random variables is calculated by a quantification of the departure from the generalized Markov property. $P\left(i_{t+1} \middle| i_t^{(k)}\right) = P\left(i_{t+1} \middle| i_t^{(k)}, j_t^{(I)}\right)$. The SE can thus be presented as

$$T_{J \to I}(k, l) = \sum P(i_{t+1}, i_t^{(k)}, j_t^{(I)}) log \frac{P\left(i_{t+1} \middle| i_t^{(k)}, j_t^{(I)}\right)}{P\left(i_{t+1} \middle| i_t^{(k)}\right)} \tag{7}$$

where $T_{J \to I}$ quantifies the information flow from J to I. Alternatively, the information flow from I to J can be deduced from $T_{I \to J}$. Quantifying the net transmission can reveal the dominant direction of the information transmission between $T_{J \to I}$ and $T_{I \to J}$.

We now discuss about the Rényi Transfer Entropy (Rényi, 1970), which follows from the SE. The RTE is dependent on a weighting factor q that is predicted to be

$$H_J^q = \frac{1}{1-q} log \sum_j P^q(j) \tag{8}$$

with $q > 0$. For $q \to 1$, RTE equates SE. For $0 < q < 1$, Consequently, occurrences with low likelihood are given more weight, while for $q > 1$ the weights benefit outcomes j with a higher original probability. Therefore, RTE permits highlighting various distribution zones based on factor q (Behrendt *et al*., 2019; Adam, 2020).

Applying the escort distribution (Beck & Schögl, 1995) $\emptyset_q(j) = \frac{p^q(j)}{\sum_j p^q(j)}$ with $q > 0$ to normalize the weighted distributions, the resultant RTE is expressed as

$$RT_{J \to I}(k, l) = \frac{1}{1-q} P(i_{t+1}, i_t^{(k)}, j_t^{(I)}) log \frac{\sum_i \emptyset_q\left(i_t^{(k)}\right) P^q\left(i_{t+1} \middle| i_t^{(k)}\right)}{\sum_{i,j} \emptyset_q\left(i_t^{(k)}, j_t^{(I)}\right) P^q\left(i_{t+1} \middle| i_t^{(k)}, j_t^{(I)}\right)} \tag{9}$$

The possibility that the RTE computation might provide adverse results must be kept in mind at all times. Given this, removing some sort of ignorance of J shows substantially greater uncertainty than when the record is known of I only would present.

In small samples, the estimates using transfer entropies could be skewed (Marschinski & Kantz, 2002). From this bias, which may be adjusted, the effective transfer entropy might be calculated as

$$ETE_{J \to I}(k, l) = T_{J \to I}(k, l) - T_{Jshuffled \to I}(k, l), \quad (10)$$

where $T_{Jshuffled \to I}(k, l)$ is a representation of the TE through a shuffled version of the time series J; i.e, through an adjustment to a random selection of observations from the actual time series J to generate a new time series, thereby destroying time series J. However, this does not ignore the reliance between the statistical reliance between J and I. $T_{Jshuffled \to I}(k, l)$ nears zero with increasing sample size. Therefore, a nonzero value of $T_{Jshuffled \to I}(k, l)$ is attributable to small samples.

To derive a bias-adjusted effective transfer entropy estimate, the small sample bias estimator is subtracted from the estimated. It consists of recurrent shuffles as well as complete reproduction of the average of the transfer entropy shuffled estimations.

Results

Preliminary statistics

The plot of the volatility indices and their fluctuations in the indices are shown in Figure 1. As the values of the indices reached their maximum with the start of the COVID-19 pandemic, it can be seen that investor panic increased dramatically at that time. All indices exhibit this trend during the pandemic's beginning. According to Gunay (2020), the pandemic's hazy depiction of economic stability and the erratic movement of asset prices at its outset led to significant adjustments in investors' portfolios to reflect their new level of risk aversion. The financial markets suffered the most losses during these times (Gunay, 2020). Therefore, it is not surprising that investor anxiety reached new heights in those markets and in those periods. The plot on the right-hand side shows evidence of volatility clusters, a regular feature of log differenced prices.

According to Table 2, the mean of the volatility indexes is close to zero. This is due to the fact that volatility changes have tail distribution and fat tails. The data collected at the 95th percentile and 5th percentile of the distribution serve as proof of this. The implication is that the tails of the distribution provide more insights into investors' behavior in these markets. We also record-high levels of dispersions daily as evidenced by the standard deviation relative to the means. The changes in the other volatility indices, aside from the Dorsey Wright Developed Market Volatility Index (VDM), exhibits positive skewness and show excess kurtosis.

This shows that, with the exception of VDM, on average a positive change in volatility indexes have taken place during the pandemic. The movement of volatility indices are typically countercyclical in nature and tend to rise during recessions while falling during periods of booms and recessions (Badshah *et al*, 2018). On average, the positive change in the volatility indices during the pandemic can be attributed to a rise in investor risk aversion as a result of elevated fear and uncertainty in the pandemic. Using the KPSS test, we are unable to disprove the null hypothesis that there is no unit root. Finally, Tsay's test for nonlinearity reveals a series of linear and non-linear combinations in the variables used in the study. This makes the RTE suitable due to its ability to account for linearities and non-linearities simultaneously.

The correlation coefficients and variances in Table 3 show that IMF-1 dominates all frequencies. As a result, we see that as IMF levels increase relative to the residual, the correlation-variance dominance decreases. Implied volatility index spikes are almost certainly mostly driven by short-term disturbances. The average period displays the respective IMFs' average frequencies (Adam *et al*., 2022).

The CMH assumes portfolio recalibration will be a characteristic feature in the short term during the pandemic, meaning that there was a high number of peaks in such periods. Moreover, the heterogeneous market hypotheses imply that investors have differing time horizons, this we reclassify as intrinsic time (see, Owusu Junior *et al*., 2021b). We group IMF-1 to IMF-4 as high frequencies, IMF-5 to IMF-7 as medium frequencies, and IMF 7-9 as low frequencies in accordance with these hypotheses and on the basis of shared characteristics of the IMFs obtained through I-CEEMDAN decomposition. The residuals reflect the deterministic long-term trend and underlying behavior of volatility series. As a result, we define periods in the pandemic up to 25 days as high frequencies, and mean periods over 25 days but less than 50 days as medium frequencies. Finally, low frequencies are defined as mean periods longer than 50 days. This is consistent with the empirical approach by Adam *et al.* (2022, Owusu Junior *et al.* (2021b), Asafo-Adjei *et al.* (2022c), Asafo-Adjei *et al.* (2022b) and Bossman *et al.* (2022a).

After having clustered the IMFs into multiple frequencies, that is, HFRQ, MFRQ, and LFRQ. Table 4 reports the respective descriptive statistics. The correlations (both Pearson correlations Kendall tau-b show that HFRQ clusters exhibit higher and more significant correlations with the original dataset. Similarly, a higher percentage of variations in investors' risk aversion occurred in average periods with high frequencies. In tandem, these highlights that short-term dynamics dominate investor preferences in these markets. This also motivates us to investigate whether investors can find safe havens by hedging their positions in the medium-frequencies, low frequencies, and the long term.

RTE framework

This section presents and discusses the results of RTE. The RTE framework produces negative (high risk) and positive (low risk) values. Critical levels between 1% and 10% are represented at the ends of the blue bars. Thus, a black bar which is either in the positive or negative regions means that there is no information flow. This suggests that any overlap at the origin is negligible or not significant. The RTE estimates are shown in Table 5, Table 6, Table 7, Table 8, Table 9 and Table 10. Their corresponding figures are presented in Figure 2 and Figure 3.

The negative information flows represent significant high-risk information flow. This means that when some ignorance is reduced by observing the changes in one variable (volatility index), a higher risk reveals itself in the near future behavior of changes in the other variable (Behrendt *et al*., 2019; Jizba *et al*., 2012). Since transfer entropy is a form of causality (see, Owusu Junior *et al*., 2021b), high-risk information flows present pertinent opportunities for portfolio diversification with such assets (see, Bossman e*t al*., 2022b; Bossman, 2021; Asafo-Adjei *et al*., 2021c). Moreover, with high risk come opportunities for high returns. Consequently, opportunities for finding profit or minizing risks diminish with positive information flows. Taking support from Ciner *et al.* (2010), who defined safe havens to include assets that are uncorrelated in stressed markets, insignificant information flows during the pandemic between markets mean low levels of market integration (see, Nyakurukwa, 2021; Lahmiri & Bekiros, 2020) and therefore can serve as safe-haven assets.

In periods dominated by high frequencies (IMF 1 — IMF 4), it can be observed that there exists a bidirectional and unidirectional flow of both significant high risk (negative) and significant low risk (positive) information between VIX and the other volatility indices. This signifies that for mean periods up to 25 days, opportunities for reducing risks with the volatility indices were apparent. Cumulatively, the HFQ summarizes the dynamic correlations between the VIX and each of the volatility indices. Overall, the plot shows that the negative information dominates the transmissions between the markets, albeit, they are largely insignificant. The results indicate that except for the Euro currency volatility index (EUVX), investors could hedge risk in the very short term with the other volatility indices. From the finding, the negative influence between the VIX and volatility indices from the several markets including commodities and stocks signifies that fluctuations in market volatilities alter the balance between risk and return or the perception of investors about future returns, thereby influencing portfolio choices.

At medium frequencies, it can also be observed that the risk and return relationships among the volatility indices also alter. However, it can be observed that the market opportunities reduce. This is evidenced by more positive information flows among the markets. Particularly, we observe that in the NASDAQ 100 (NVX), CAC 40 index (index for Paris stock market), the emerging market volatility index (VXEM), Russel 2000 volatility index (RVX), and volatility index for German stock market (VDAX). Similarly, it is observed at low frequencies that the net information flow between CAC 40 index, energy sector volatility index (VXES), and Euro currency volatility index (EUVX) is positive and significant. This means that no opportunities for minimizing risk can emerge in any investment between VIX and each of the aforementioned volatility indices.

The residuals represent the deterministic long-term trend. We observe that there exists a bidirectional flow of negative information between each of the indices and the VIX. It can also be observed that the information flows from VIX to the other indices are stronger.

Further, we vary the tails of the distribution from the 50th quantile to other quantiles (0.05, 0.3, 0.8, and 0.95). The lower tails (q = 5 and q =30) represent low levels of investor risk aversion (Barson *et al*., 2022; Archer *et al*., 2022). We find that opportunities for hedging risks during the pandemic increase marginally in the short term (at high frequencies). Unlike the information flows that exist at the median quantile, investors can find safe haven properties exist between the VIX and all the volatility indices in the short term. In the medium term, however, the profit opportunities at the 30th quantile are identical to those that exist at the 50th quantile. However, it can be observed that only NASDAQ 100 (NVX) is not a safe haven for VIX at the 5th quantile. At lower frequencies, the results also indicate that the net information flow between each CAC 40 index and energy sector volatility index (VXES) with VIX is significant and positive, therefore diminishing any safe haven benefits. At the upper tails of the distribution (q = 0.8 and q= 0.95), the study reports that positive information flows among the markets increase substantially. This signifies that the benefits of hedging with most of the volatility indices and the VIX reduces substantially at medium frequencies and low frequencies. Consistently across all quantiles, it can be observed that a bidirectional flow of negative information exists between each of the volatility indices and VIX at their residual.

Discussion

Findings from the study indicate that the dynamics of information flows between VIX and the fifteen volatility indices are time-varying. This underscores the heterogeneous and adaptive nature of financial markets and market participants as found by prior studies (Asafo-Adjei *et al*., 2021b; Boateng *et al*., 2022a; Bossman *et al*., 2022b; Bossman, 2021; Asafo-Adjei *et al*., 2022a; Agyei *et al*., 2022, etc.). It is increasingly obvious that opportunities for profits and risk management varies across different time horizons and depends on the levels of investor risk aversion. In the high frequencies, we notice higher opportunities to hedge risks. However, this reduces marginally in the low and medium frequencies.

Due to the coronavirus pandemic, which increased uncertainties in the prices of financial assets (Gunay, 2020) and accelerated the flight to safety (Bossman *et al*., 2022b), financial markets may undergo mutation and adaptations. Thus, opportunities for profits may evolve and investors may also have to adapt to survive according to their varying risk appetites. This is consistent with the adaptive market hypothesis of Lo (2004). Our finding also divulges that short-term investors who seek to minimize losses with volatility indices may completely shun the Euro currency index (EUVX). However, slight opportunities for diversification, depending on an investor's risk appetite emerge in the medium frequencies and further diminishes at low frequencies. Thus, we document that market opportunities also evolve based on investors' horizons, consistent with the heterogeneous market hypothesis of Müller *et al.* (1993). Finally, the findings show that opportunities for hedging with the volatility indices evolve not only according to the heterogeneous targets/expectations of market participants but also to the varying levels of investor risk aversion.

The findings reveal that opportunities for hedging with the volatility indices minimize according to increasing levels of risk aversion. The amount of information transmission between volatility indices likely changes as markets continue to adjust and is compounded by investors' rational, if irrational, search for competing risks and reward preferences. Financial asset price declines during a pandemic may have an impact on investors' portfolio decisions by changing the trade-off between risk and return or providing a glimpse into how the market may behave in the future. According to the CMH of Owusu Junior *et al*. (2021), this leads to a recalibration of investor portfolios to reflect their revised competing risk and return preferences.

In addition, our results divulge that regardless of the levels of investor risk aversion, the volatility indices act as effective hedges in the long term. While we expect the markets to be integrated into the long-term, this is not startling given that the residuals are driven by fundamentals (Owusu Junior *et al*., 2021). This presupposes that the volatility dynamics in those markets will be driven by asset-specific factors.

Moreover, the finding lend support to the conclusion that hedging opportunities are non-linear over investors' time horizons. The conclusion is premised on the evidence that investor opportunities with the given set of volatility indices are higher in high frequencies and reduces in medium and low frequencies but amplify in the long term. The intrinsic uncertainty in economic fundamentals at the start of the pandemic increases noise (evidenced by high levels of variations and peak periods in the short term of the pandemic, see Table 3). Therefore, transitory upward or downward price movements that deviate from fundamentals may be prevalent, especially when a significant enough percentage of traders believe in those bubbles. Since herding behaviors are likely to be common in the pandemic (Espinosa-Méndez & Arias, 2021), it is not surprising that the information flows between VIX and the other volatility indices deviate from fundamentals in high frequencies, low frequencies, and medium frequencies.

However, over time, investors continue to update their beliefs (Hommes, 2001) and as countries minimize lockdown restrictions, and life returns to normalcy, this drives down investor fear and risk aversion (see, Figure 1 which shows declining risk aversion over time compared to the start of the pandemic), and opportunities in the market and information flow may mimic the deterministic long-term trend (driven by fundamentals than irrational fear). This makes global financial markets “non-linear heterogeneous evolutionary systems.”

Conclusions

We assessed the multi-frequency information flow between VIX and implied volatility indices of other global financial markets. In line with the heterogeneous nature of market participants, and to deal with noise that is inherent in volatility indices, we employed the ICEEMDAN-based decomposition on a sample that spanned within the COVID-19 window. The multiple frequencies from the decomposed series were clustered into high, medium, and low frequencies for IMFs 1–9 and the residual. To address problems of non-linearity, non-stationarity, and asymmetric relationships that are apparent in financial time series data, the study adopted the Rényi transfer entropy. We set q to 0.05, 0.3, 0.5, 0.8, and 0.95 to account for all events, particularly tail events, and explain the dynamics of the markets according to varying levels of investor risk aversion.

The properties of the IMFs reveal that changes in prices of the implied volatility indices are dominated by short-lived fluctuations, evidenced by the correlation coefficients and variations. This may be due to the initial stages of the pandemic which increased the levels of investors' risk aversion. At such levels of investor risk aversion (upper quantiles), we document that the opportunities for diversification minimize, relative to the lower quantiles. The correlation coefficients and variations decline with increasing IMFs and reduce substantially for the residuals. This supports the assertion that markets and market participants undergo mutation and evolution, partly due to the experiences of the participants and conditions in the business environment, and therefore, the degree of efficiency of the market varies over time, consistent with the adaptive market hypothesis.

The study documents that in the long-term, there exists a bidirectional flow of only low-risk information. In the residuals, we report that the dominance of the VIX in transmitting negative information in the long term. While this implies that elimination of some ignorance of historical changes in the VIX presents high-risk in forecasting future changes in the other volatility indices. With high risks and uncertainties emerge the possibility of high return. As a consequence, investors may consider diversification with the VIX and other volatility indices profitable. The negative information flows are also indicative that these markets can act as a safe haven to the VIX in times of the pandemic (see, Asafo-Adjei *et al*., 2022c; Bossman, 2021; Owusu Junior *et al.*, 2021a). Therefore, the study recommends that that the VIX can hedge effectively other market implied volatilities in the long-term dynamics of the COVID-19 pandemic. This feature of the deterministic long-term trend is not evident for the other frequencies (high, medium, and low). We report a bidirectional flow of both high-risk and low-risk information between the VIX and the volatility indices. This suggests that investors must undertake active portfolio rebalancing to maximize their returns, consistent with their levels of risk aversion as profit opportunities are also minimized with increasing investor risk aversion.

At varying levels of investor risk aversion, we document that the opportunities for diversification are higher in low frequencies, but reduce in medium and high frequencies, and rise again in the long-term. This makes global financial markets "non-linear heterogeneous evolutionary systems." In another vein, our findings signify that those investors who delayed their investments in the volatility indices effectively managed risks in their portfolios. This partly amplifies the delayed volatility of market competitiveness and external shocks (DVMCES) hypothesis espoused in the study of Asafo-Adjei *et al*. (2022c).

Since correlations among markets can change, which may also alter the nature of information flows among markets, future studies can conduct a comparative assessment of the dynamics of the markets before the pandemic. Further, the dynamics of financial markets may also not be constant over time, not only frequencies. Alternative studies can employ time-frequency methodologies such as wavelet coherence to assess the phenomenon. This is because the current study only assesses the phenonomenon in frequency domains. A further weakness of this study is that it only considers the bidirectional relationship between VIX and each of the other implied volatility indices but does not probe beyond to examine how all of these variables are integrated. Thus, it is possible that the relationships between two set of volatility indices could be driven by another third force, which is not considered in this study. Consequently, these findings should be assimilated with caution when applied in practice.

References

Adam, A. M. (2020). Susceptibility of stock market returns to international economic policy: evidence from effective transfer entropy of Africa with the implication for open innovation. *Journal of Open Innovation: Technology, Market, and Complexity*, *6*(3), 71. doi: 10.3390/joitmc6030071.

Adam, A. M., Kyei, K., Moyo, S., Gill, R., & Gyamfi, E. N. (2022). Similarities in Southern African Development Community (SADC) exchange rate markets structure: evidence from the ensemble empirical mode decomposition. *Journal of African Business*, *23*(2), 516–530.

Agyei, S. K., Adam, A. M., Bossman, A., Asiamah, O., Owusu Junior, P., Asafo-Adjei, R., & Asafo-Adjei, E. (2022). Does volatility in cryptocurrencies drive the interconnectedness between the cryptocurrencies market? Insights from wavelets. *Cogent Economics & Finance*, *10*(1), 2061682. doi: 10.1080/23322039.2022.2061682.

Archer, C., Owusu Junior, P., Adam, A. M., Asafo-Adjei, E., & Baffoe, S. (2022). Asymmetric dependence between exchange rate and commodity prices in Ghana. *Annals of Financial Economics*, *17*(2) 2250012. doi: 10.1142/S2010495222500129.

Asafo-Adjei, E., Adam, A. M., & Darkwa, P. (2021a). Can crude oil price returns drive stock returns of oil producing countries in Africa? Evidence from bivariate and multiple wavelet. *Macroeconomics and Finance in Emerging Market Economies*. Advance online publication. doi: 10.1080/17520843.2021.1953864.

Asafo-Adjei, E., Adam, A. M., Adu-Asare Idun, A., & Ametepi, P. Y. (2022a). Dynamic interdependence of systematic risks in emerging markets economies: a recursive-based frequency-domain approach. *Discrete Dynamics in Nature and Society*, *2022*, 1139869. doi: 10.1155/2022/1139869.

Asafo-Adjei, E., Adam, A. M., Owusu Junior, P., Akorsu, P. K., & Arthur, C. L. (2022b). A CEEMDAN-based entropy approach measuring multiscale information flow between macroeconomic conditions and stock returns of BRICS. *Complexity*, *2022*, 1–24. doi: 10.1155/2022/7871109.

Asafo-Adjei, E., Boateng, E., Isshaq, Z., Idun, A. A. A., Owusu Junior, P., & Adam, A. M. (2021b). Financial sector and economic growth amid external uncertainty shocks: insights into emerging economies. *Plos one*, *16*(11), e0259303. doi: 10.1371/journal.pone.0259303.

Asafo-Adjei, E., Frimpong, S., Owusu Junior, P., Adam, A. M., Boateng, E., & Ofori Abosompim, R. (2022). Multi-frequency information flows between global commodities and uncertainties: evidence from COVID-19 pandemic. *Complexity*, *2022*, 6499876. doi: 10.1155/2022/6499876.

Asafo-Adjei, E., Owusu Junior, P., & Adam, A. M. (2021c). Information flow between global equities and cryptocurrencies: a VMD-based entropy evaluating shocks from COVID-19 pandemic. *Complexity, 2021,* 4753753. doi: 10.1155/2021/4753753.

Badshah, I. U. (2018). Volatility spillover from the fear index to developed and emerging markets. *Emerging Markets Finance and Trade*, *54*(1), 27–40. doi: 10.1080/1540496X.2016.1220294.

Badshah, I., Bekiros, S., Lucey, B. M., & Uddin, G. S. (2018). Asymmetric linkages among the fear index and emerging market volatility indices. *Emerging Markets Review*, *37*, 17–31. doi: 10.1016/j.ememar.2018.03.002.

Balcilar, M., & Demirer, R. (2015). Effect of global shocks and volatility on herd behavior in an emerging market: evidence from Borsa Istanbul. *Emerging Markets Finance and Trade*, *51*(1), 140–159. doi: 10.1080/1540496X.2015.1011520.

Barson, Z., Junior, P. O., Adam, A. M., & Asafo-Adjei, E. (2022). Connectedness between gold and cryptocurrencies in COVID-19 pandemic: a frequency-dependent asymmetric and causality analysis. *Complexity*, *2022,* 7648085. doi: 10.1155/2022/7648085.

Beck, C, & Schögl, F. (1995). *Thermodynamics of chaotic systems: an introduction*. Cambridge: Cambridge University Press.

Behrendt, S., Dimpfl, T., Peter, F. J., & Zimmermann, D. J. (2019). RTransferEntropy—quantifying information flow between different time series using effective transfer entropy. *SoftwareX*, *10*, 100265. doi: 10.1016/j.softx.2019.100265.

Boateng, E., Adam, A. M., & Owusu Junior, P. (2021). Modelling the heterogeneous relationship between the crude oil implied volatility index and African stocks in the coronavirus pandemic. *Resources policy*, *74*, 102389. doi: 10.1016/j.resourpol.2021.102389.

Boateng, E., Asafo-Adjei, E., Addison, A., Quaicoe, S., Yusuf, M. A., & Adam, A. M. (2022a). Interconnectedness among commodities, the real sector of Ghana and external shocks. *Resources Policy*, *75*, 102511. doi: 10.1016/j.resourpol.2021.102511.

Boateng, E., Owusu Junior, P., Adam, A. M., Abeka Jr, M., Qabhobho, T., & Asafo-Adjei, E. (2022b). Quantifying information flows among developed and emerging equity markets. *Mathematical Problems in Engineering*, 2022, 2462077. doi: 10.1155/2022/2462077.

Bossman, A. (2021). Information flow from COVID-19 pandemic to Islamic and conventional equities: an ICEEMDAN-induced transfer entropy analysis. *Complexity*, *2021*, 4917051. doi: 10.1155/2021/4917051.

Bossman, A., Agyei, S. K., Owusu Junior, P., Agyei, E. A., Akorsu, P. K., Marfo-Yiadom, E., & Amfo-Antiri, G. (2022a). Flights-to-and-from-quality with Islamic and conventional bonds in the COVID-19 pandemic era: ICEEMDAN-based transfer entropy. *Complexity*, *2022*, 1027495. doi: 10.1155/2022/1027495.

Bossman, A., Owusu Junior, P., & Tiwari, A. K. (2022b). Dynamic connectedness and spillovers between Islamic and conventional stock markets: time-and frequency-domain approach in COVID-19 era. *Heliyon*, *8*(4), e09215. doi: 10.1016/j.heliyon.2022.e09215.

Bulathsinhalage, S., & Pathirawasam, C. (2017). The effect of corporate governance on firms' capital structure of listed companies in Sri Lanka. *Journal of Competitiveness*, *9*(2), 19–33. doi: 10.7441/joc.2017.02.02.

Bui, T. D., & Bui, H. T. M. (2020). Threshold effect of economic openness on bank risk-taking: evidence from emerging markets. *Economic Modelling*, *91*, 790–803. doi: 10.1016/j.econmod.2019.11.013.

Chen, J. H., & Huang, Y. F. (2014). Long memory and structural breaks in modelling the volatility dynamics of VIX-ETFs. *International Journal of Business, Economics and Law*, *4*(1), 54–63.

Cheuathonghua, M., Padungsaksawasdi, C., Boonchoo, P., & Tongurai, J. (2019). Extreme spillovers of VIX fear index to international equity markets. *Financial Markets and Portfolio Management*, *33*(1), 1–38. doi: 10.1007/s11408-018-0323-6.

Ciner, C., Gurdgiev, C., & Lucey, B. M. (2010). Hedges and safe havens: an examination of stocks, bonds, oil, gold and the dollar. *International Review of Financial Analysis*, *29*, 202–211. doi: 10.1016/j.irfa.2012.12.001.

Colominas, M. A., Schlotthauer, G., & Torres, M. E. (2014). Improved complete ensemble EMD: a suitable tool for biomedical signal processing. *Biomedical Signal Processing and Control*, *14*, 19–29. doi: 10.1016/j.bspc.2014.06.009.

Del Castillo Olivares, A. F., Kumiega, A., Sterijevski, G., & Van Vliet, B. (2018). An empirical study of volatility spillover worldwide. *Wilmott*, *2018*(95), 48–59. doi: 10.1002/wilm.10675.

Dimpfl, T., & Peter, F. J. (2014). The impact of the financial crisis on transatlantic information flows: an intraday analysis. *Journal of International Financial Markets, Institutions and Money*, *31*, 1–13. doi: 10.1016/j.intfin.2014.03.004.

Dutta, A., Nikkinen, J., & Rothovius, T. (2017). Impact of oil price uncertainty on middle east and african stock markets. *Energy*, *123*, 189–197. doi: 10.1016/j.energy.2017.01.126.

Espinosa-Méndez, C., & Arias, J. (2021). COVID-19 effect on herding behaviour in European capital markets. *Finance Research Letters*, *38*, 101787. doi: 10.1016/j.frl.2020.101787.

Flandrin, P., Goncalves, P., & Rilling, G. (2004). Detrending and denoising with empirical mode decompositions. In *2004 12th European signal processing conference*. Vienna: *IEEE,* 1581–1584.

Gallegati, M. (2012). A wavelet-based approach to test for financial market contagion. *Computational Statistics & Data Analysis*, *56*(11), 3491–3497. doi: 10.1016/j.csda.2010.11.003.

Gunay, S. (2020). A new form of financial contagion: Covid-19 and stock market responses. *SSRN, 3584243*. doi: 10.2139/ssrn.3584243.

Hartley, R. V. (1928). Transmission of information 1. *Bell System Technical Journal*, *7*(3), 535–563. doi: 10.1002/j.1538-7305.1928.tb01236.x.

Hommes, C. H. (2001). Financial markets as nonlinear adaptive evolutionary systems. *Quantitative Finance*, *1*(1), 149. doi: 10.1088/1469-7688/1/1/311.

Huang, N. E., Shen, Z., Long, S. R., Wu, M. C., Shih, H. H., Zheng, Q., Yen, N-C., Tung, C.C., & Liu, H. H. (1998). The empirical mode decomposition and the Hilbert spectrum for nonlinear and non-stationary time series analysis. *Proceedings of the Royal Society of London. Series A: Mathematical, Physical and Engineering Sciences*, *454*(1971), 903–995. doi: 10.1098/rspa.1998.0193.

Jizba, P., Kleinert, H., & Shefaat, M. (2012). Rényi's information transfer between financial time series. *Physica A: Statistical Mechanics and its Applications*, *391*(10), 2971–2989. doi: 10.1016/j.physa.2011.12.064.

Khoury, T. A., Junkunc, M., & Mingo, S. (2015). Navigating political hazard risks and legal system quality: venture capital investments in Latin America. *Journal of Management*, *41*(3), 808–840. doi: 10.1177/0149206312453737.

Kullback, S., & Leibler, R. A. (1951). On information and sufficiency. *Annals of Mathematical Statistics*, *22*(1), 79–86.

Lahmiri, S., & Bekiros, S. (2020). Renyi entropy and mutual information measurement of market expectations and investor fear during the COVID-19 pandemic. *Chaos, Solitons & Fractals*, *139*, 110084. doi: 10.1016/j.chaos.2020.110084y.

Law, S. H., & Habibullah, M. S. (2009). The determinants of financial development: institutions, openness and financial liberalisation. *South African Journal of Economics*, *77*(1), 45–58. doi: 10.1111/j.1813-6982.2009.01201.x.

Le, T. H., Kim, J., & Lee, M. (2016). Institutional quality, trade openness, and financial sector development in Asia: an empirical investigation. *Emerging Markets Finance and Trade*, *52*(5), 1047–1059. doi: 10.1080/1540496X.2015.1103138.

Lekhal, M., & El Oubani, A. (2020). Does the adaptive market hypothesis explain the evolution of emerging markets efficiency? Evidence from the Moroccan financial market. *Heliyon*, *6*(7), e04429. doi: 10.1016/j.heliyon.2020.e04429

Li, T., Qian, Z., & He, T. (2020). Short-term load forecasting with improved CEEMDAN and GWO-based multiple kernel ELM. *Complexity*, *2020,* 1209547. doi: 10.1155/2020/1209547.

Lim, K. P., & Kim, J. H. (2011). Trade openness and the informational efficiency of emerging stock markets. *Economic Modelling*, *28*(5), 2228–2238. doi: 10.1016/j.econmod.2011.06.004.

Lo, A. W. (2004). The adaptive markets hypothesis. *Journal of Portfolio Management*, *30*(5), 15–29. doi: 10.3905/jpm.2004.442611.

Marschinski, R., & Kantz, H. (2002). Analysing the information flow between financial time series. *European Physical Journal B-Condensed Matter and Complex Systems*, *30*(2), 275–281. doi: 10.1140/epjb/e2002-00379-2.

Müller, U. A., Dacorogna, M. M., Davé, R. D., Pictet, O. V., Olsen, R. B., & Ward, J. R. (1993). Fractals and intrinsic time: a challenge to econometricians. Unpublished manuscript, Olsen & Associates, Zürich.

Nyakurukwa, K. (2021). Information flow between the Zimbabwe Stock Exchange and the Johannesburg Stock Exchange: a transfer entropy approach. *Organizations and Markets in Emerging Economies*, *12*(24), 353–376. doi: 10.15388/omee.2021.12.60.

Owusu Junior, P., Adam, A. M., Asafo-Adjei, E., Boateng, E., Hamidu, Z., & Awotwe, E. (2021a). Time-frequency domain analysis of investor fear and expectations in stock markets of BRIC economies. *Heliyon*, *7*(10), e08211. doi: 10.1016/j.heliyon.2021.e08211.

Owusu Junior, P., Frimpong, S., Adam, A. M., Agyei, S. K., Gyamfi, E. N., Agyapong, D., & Tweneboah, G. (2021b). COVID-19 as information transmitter to global equity markets: evidence from CEEMDAN-based transfer entropy approach. *Mathematical Problems in Engineering*, *2021,* 8258778. doi: 10.1155/2021/8258778.

Peng, Y., & Ng, W. L. (2012). Analysing financial contagion and asymmetric market dependence with volatility indices via copulas. *Annals of Finance*, *8*(1), 49–74. doi: 10.1007/s10436-011-0181-y.

Ramsey, J. B., & Lampart, C. (1998). The decomposition of economic relationships by time scale using wavelets: expenditure and income. *Studies in Nonlinear Dynamics & Econometrics*, *3*(1), 23–42. doi: 10.2202/1558-3708.1039.

Rényi, A. (1970). *Probability theory*. Amsterdam: North-Holland Publ. Co.

Sarwar, G. (2019). Transmission of risk between US and emerging equity markets. *Emerging Markets Finance and Trade*, *55*(5), 1171–1183. doi: 10.1080/1540496X.2018.1468248.

Shannon, C. E. (1948). A mathematical theory of communication. *Bell System Technical Journal*, *27*(3), 379–423. doi: 10.1002/j.1538-7305.1948.tb01338.x.

Smales, L. A. (2022). Spreading the fear: the central role of CBOE VIX in global stock market uncertainty. *Global Finance Journal*, *51*, 100679. doi: 10.1016/j.gfj.2021.100679.

Tissaoui, K., & Zaghdoudi, T. (2021). Dynamic connectedness between the US financial market and Euro-Asian financial markets: testing transmission of uncertainty through spatial regressions models. *Quarterly Review of Economics and Finance*, *81*, 481–492. doi: 10.1016/j.qref.2020.10.020.

Torres, M. E., Colominas, M. A., Schlotthauer, G., & Flandrin, P. (2011). A complete ensemble empirical mode decomposition with adaptive noise. In *2011 IEEE international conference on acoustics, speech and signal processing (ICASSP). IEEE,* 4144–4147.

Valaskova, K., Kliestik, T., & Gajdosikova, D. (2021). Distinctive determinants of financial indebtedness: evidence from Slovak and Czech enterprises. *Equilibrium. Quarterly Journal of Economics and Economic Policy*, *16*(3), 639–659. doi: 10.24136/eq.2021.023.

Wu, Z., & Huang, N. E. (2009). Ensemble empirical mode decomposition: a noise-assisted data analysis method. *Advances in Adaptive Data Analysis*, *1*(1), 1–41. doi: 10.1142/S1793536909000047.

Annex

Table 1. Samples of volatility indices

Volatilities	**Codes**
CBOE Euro Currency Volatility	EUVX
CBOE Gold Volatitity	GVX
CBOE NASDAQ 100 Volatility	NVX
CBOE Crude Oil Volatility	OVX
CBOE Russell 2000 Volatility	RVX
DAX New Volatility	VDAX
DJIA Volatility	VDJIA
Dorsey Wright Developed Market Momentum and Low Volatility	VDM
HSI Volatility	VHSI
CBOE VIX	VIX
CAC 40 VIX	VIXCAC
STOXX 50 Volatility VSTOXX	VSTOXX
CBOE Vix Volatility_VVIX	VVIX
CBOE Emerging Markets Etf Volitlity	VXEM
CBOE Energy Sector Etf Volitlity	VXES
CBOE OEX Implied Volatility	VXOEX

Source: own calculations based on data obtained from investing.com.

Table 2. Descriptive statistics

	Mean	**95th**	**5th**	**Std. Dev.**	**Skewness**	**Kurtosis**	**Jarque-Bera**	**KPSS**	**Tsay**
EUVX	0.0012	0.1024	-0.1122	0.0702	0.4121	7.5606	210.3089***	0.2936	0.6050[1]
GVX	0.0011	0.1168	-0.0972	0.0711	0.3994	5.1405	51.1078***	0.2562	0.3114[0]
NVX	0.0009	0.1477	-0.1052	0.0837	0.8505	8.8303	361.1741***	0.2300	1.6880[1]
OVX	0.0006	0.1527	-0.1371	0.1156	1.3816	22.7458	3892.4800***	0.1586	4.6420***[2]
RVX	0.0018	0.1444	-0.0999	0.0813	1.1367	7.2812	230.0786***	0.2231	2.9190***[9]
VDAX	0.0008	0.1542	-0.1025	0.0808	1.1827	5.4493	113.5261***	0.2617	0.4436[1]
VDJIA	0.0011	0.1496	-0.0853	0.0771	1.0879	6.0504	137.4643***	0.2337	0.8554[0]
VDM	0.0003	0.0186	-0.0226	0.0198	-1.1379	15.6494	1617.4500***	0.3787	7.1740***[7]
VHSI	0.0002	0.1441	-0.1248	0.0827	1.1427	8.0327	299.1469***	0.0666	0.1039[0]
VIX	0.0012	0.1892	-0.1146	0.0946	1.4024	6.9005	225.9979***	0.1639	2.1760**[3]
VIXCAC	0.0011	0.1600	-0.1275	0.0923	0.6812	5.4157	75.3143***	0.2182	1.3990**[12]
VSTOXX	0.0011	0.1827	-0.1164	0.0895	1.1309	5.1445	95.1202***	0.2102	6.0370***[0]
VVIX	0.0011	0.0883	-0.0657	0.0474	0.9830	5.7408	111.4040***	0.0586	0.1807[0]
VXEM	0.0005	0.1602	-0.1369	0.0938	0.4919	5.6407	77.7565***	0.1160	1.4000[2]
VXES	0.0023	0.1375	-0.0948	0.0756	1.2906	7.0125	222.8921***	0.2841	1.9800[2]
VXOEX	0.0005	0.1874	-0.1491	0.1122	0.8769	5.9742	116.7349***	0.1430	2.1790[2]

Note: *.**,*** designates significance levels at 10%, 5% and 1% respectively. Values in brackets indicate automatically determined order of the autoregressive function

Source: own calculations based on data obtained from investing.com, R programming version 4.2.0.

Table 3. Volatilities measures of IMFs obtained through I-CEEMDAN

	IMF1	IMF2	IMF3	IMF4	IMF5	IMF6	IMF7	IMF8	IMF9	Residual
					EUVX					
μ	2.61	4.90	8.70	14.69	26.11	47	58.75	117.50	78.33	
ρ	0.73***	0.45***	0.29***	0.25***	0.23***	0.15**	0.12**	0.09*	-0.11	-0.10
σ_1^2	61.55%	21.78%	8.70%	4.95%	2.31%	2.29%	1.83%	0.32%	0.01%	0.01%
σ_2^2	61.55%	21.78%	8.70%	4.95%	2.31%	2.29%	1.83%	0.32%	0.01%	0.01%
					GVX					
μ	2.50	5.47	9.97	18.08	33.57	47.00	78.33	78.33	117.50	
ρ	0.75***	0.55***	0.27***	0.16**	0.14**	0.18***	0.04	0.07	0.08	0.09*
σ_1^2	54.08%	23.69%	8.61%	4.76%	5.01%	3.12%	0.31%	0.06%	0.04%	0.01%
σ_2^2	54.08%	23.69%	8.61%	4.76%	5.01%	3.12%	0.31%	0.06%	0.04%	0.01%
					NVX					
μ	2.61	5.34	9.79	19.58	29.38	47.00	58.75	117.50	78.33	
ρ	0.78***	0.46***	0.30***	0.20***	0.19***	0.18***	0.13**	0.07	-0.08	0.07
σ_1^2	63.57%	17.74%	8.27%	4.17%	1.08%	0.90%	1.35%	0.67%	0.01%	0.01%
σ_2^2	63.57%	17.74%	8.27%	4.17%	1.08%	0.90%	1.35%	0.67%	0.01%	0.01%
					OVX					
μ	2.70	5.88	9.79	15.67	26.11	47.00	58.75	78.33	117.50	
ρ	0.70***	0.51***	0.27***	0.18***	0.19***	0.14**	0.11*	0.04	0.07	0.07
σ_1^2	54.97%	25.97%	13.06%	4.89%	4.13%	2.08%	3.74%	0.38%	0.23%	0.03%
σ_2^2	54.97%	25.97%	13.06%	4.89%	4.13%	2.08%	3.74%	0.38%	0.23%	0.03%
					RVX					
μ	2.67	5.60	10.22	19.58	29.38	39.17	58.75	117.50	117.50	
ρ	0.81***	0.42***	0.30***	0.23***	0.24***	0.17***	0.08	0.08	0.09*	0.07
σ_1^2	65.35%	14.21%	7.89%	4.32%	0.92%	1.36%	0.12%	0.32%	0.02%	0.01%
σ_2^2	65.35%	14.21%	7.89%	4.32%	0.92%	1.36%	0.12%	0.32%	0.02%	0.01%
					VDAX					
μ	2.67	4.90	9.04	16.79	26.11	39.17	58.75	117.50	117.50	
ρ	0.75***	0.52***	0.42***	0.26***	0.23***	0.20***	0.15**	0.13**	0.09*	-0.11
σ_1^2	48.33%	13.25%	13.74%	4.41%	2.56%	1.34%	0.28%	0.34%	0.01%	0.01%
σ_2^2	48.33%	13.25%	13.74%	4.41%	2.56%	1.34%	0.28%	0.34%	0.01%	0.01%

Table 3. Continued

	IMF1	IMF2	IMF3	IMF4	IMF5	IMF6	IMF7	IMF8	IMF9	Residual
					VDJIA					
μ	2.58	4.70	9.40	15.67	29.38	39.17	58.75	58.75	78.33	
ρ	0.76***	0.52***	0.39***	0.28***	0.20***	0.20***	0.15**	0.08	0.06	0.11**
σ_1^2	53.42%	10.91%	9.15%	4.89%	2.54%	2.89%	0.95%	0.72%	0.41%	0.01%
σ_2^2	53.42%	10.91%	9.15%	4.89%	2.54%	2.89%	0.95%	0.72%	0.41%	0.01%
					VDM					
μ	2.70	5.88	10.22	16.79	21.36	39.17	78.33	78.33	117.50	
ρ	0.71***	0.38***	0.30***	0.24***	0.22***	0.21***	0.13**	0.10*	0.12**	0.13**
σ_1^2	49.68%	31.56%	22.42%	7.50%	1.75%	1.15%	1.20%	0.39%	0.08%	0.03%
σ_2^2	49.68%	31.56%	22.42%	7.50%	1.75%	1.15%	1.20%	0.39%	0.08%	0.03%
					VHSI					
μ	2.64	5.73	11.75	19.58	29.38	39.17	58.75	117.50	117.50	
ρ	0.74***	0.48***	0.34***	0.18***	0.20***	0.10*	0.06	0.06	0.04	-0.03
σ_1^2	60.42%	26.25%	13.52%	1.92%	0.85%	0.22%	0.45%	0.19%	0.01%	0.01%
σ_2^2	60.42%	26.25%	13.52%	1.92%	0.85%	0.22%	0.45%	0.19%	0.01%	0.01%
					VIX					
μ	2.58	5.22	9.79	18.08	29.38	39.17	47.00	78.33	78.33	
ρ	0.78***	0.43***	0.31***	0.21***	0.24***	0.17***	0.14**	0.08	-0.09	-0.06
σ_1^2	62.38%	14.31%	8.64%	4.24%	3.93%	1.25%	0.71%	0.93%	0.01%	0.01%
σ_2^2	62.38%	14.31%	8.64%	4.24%	3.93%	1.25%	0.71%	0.93%	0.01%	0.01%
					VIXCAC					
μ	2.73	4.80	10.22	19.58	29.38	47.00	58.75	117.50	117.50	
ρ	0.79***	0.47***	0.26***	0.21***	0.19***	0.18***	0.13**	0.09*	0.09*	-0.08
σ_1^2	61.65%	14.02%	12.37%	4.79%	2.36%	1.56%	0.26%	0.35%	0.01%	0.01%
σ_2^2	61.65%	14.02%	12.37%	4.79%	2.36%	1.56%	0.26%	0.35%	0.01%	0.01%
					VSTOXX					
μ	2.73	5.11	9.04	16.79	26.11	39.17	58.75	58.75	117.50	
ρ	0.75***	0.52***	0.43***	0.29***	0.18***	0.23***	0.16**	0.09*	0..09*	0.09*
σ_1^2	47.62%	13.99%	15.09%	3.64%	1.51%	0.95%	0.64%	0.06%	0.20%	0.01%
σ_2^2	47.62%	13.99%	15.09%	3.64%	1.51%	0.95%	0.64%	0.06%	0.20%	0.01%

Table 3. Continued

	IMF1	IMF2	IMF3	IMF4	IMF5	IMF6	IMF7	IMF8	IMF9	Residual
					VVIX					
μ	2.61	5.47	10.22	16.79	29.38	47.00	58.75	78.33	117.50	
ρ	0.72***	0.53***	0.34***	0.25***	0.20***	0.15**	0.06	0.06	0.03	-0.01
σ_1^2	53.25%	18.94%	9.37%	5.64%	6.59%	2.40%	0.36%	0.21%	0.01%	0.01%
σ_2^2	53.25%	18.94%	9.37%	5.64%	6.59%	2.40%	0.36%	0.21%	0.01%	0.01%
					VXEM					
μ	2.70	5.73	11.75	23.50	39.17	47.00	58.75	78.33	78.33	
ρ	0.77***	0.42***	0.31***	0.16**	0.17**	0.10*	0.11**	0.06	0.04	-0.07
σ_1^2	64.27%	22.69%	12.28%	5.37%	2.67%	0.30%	0.06%	0.15%	0.07%	0.01%
σ_2^2	64.27%	22.69%	12.28%	5.37%	2.67%	0.30%	0.06%	0.15%	0.07%	0.01%
					VXES					
μ	2.67	5.00	10.22	18.08	29.38	47.00	58.75	78.33	78.33	
ρ	0.72***	0.50***	0.34***	0.27***	0.20***	0.23***	0.19***	0.09*	0.08	-0.12
σ_1^2	52.78%	21.44%	8.19%	3.86%	1.04%	3.02%	1.36%	0.58%	0.01%	0.01%
σ_2^2	52.78%	21.44%	8.19%	3.86%	1.04%	3.02%	1.36%	0.58%	0.01%	0.01%
					VXOEX					
μ	2.55	5.34	10.22	21.36	29.38	47.00	58.75	58.75	78.33	
ρ	81.62***	0.44***	0.30***	0.22***	0.18***	0.17***	0.12**	0.05	0.03	0.07
σ_1^2	64.98%	14.20%	6.42%	4.94%	1.01%	1.01%	1.13%	0.50%	0.10%	0.01%
σ_2^2	64.98%	14.20%	6.42%	4.94%	1.01%	1.01%	1.13%	0.50%	0.10%	0.01%

Note: μ, ρ, σ_1^2 and σ_2^2 denote mean period, Pearson product-moment correlations, variance as % of observed, and variance as % of the sum of all IMFs and Residue. : [*, **] show significance levels at 5-, and 1 percent respectively. Table 3 presents the features of the decomposed data. We report the mean period (μ) measured by the total number of points divided by the number of peaks. This means that the value of the μ is indirectly related to the level of frequency. The Pearson correlation coefficients (ρ) are also reported computed as the correlation between each IMF and the original/observed volatility indices. The variance proportion of each IMF and the residue to the variance in the original data (σ_1^2) as well as the variance proportion of each IMF to the total variance in the decomposed data (σ_2^2). The latter should mainly corroborate with σ_1^2.

Source: own calculations based on data obtained from investing.com, R programming version 4.2.0.

Table 4. Descriptive statistics of the reconstructed series and the residue obtained through I-CEEMDAN

Volatilities	Pearson correlation coefficient				Kendall tau-b			
	HFRQ	**MFRQ**	**LFRQ**	**RESID**	**HFRQ**	**MFRQ**	**LFRQ**	**RESID**
EUVX	0.97***	0.25***	0.15**	-0.10	0.84***	0.16***	0.07*	-0.05
GVX	0.95***	0.23***	0.08	0.09*	0.83***	0.11**	0.02	0.03
NVX	0.97***	0.22***	0.13**	0.07	0.82***	0.13***	0.05	-0.01
OVX	0.95***	0.21***	0.16**	0.07	0.71***	0.11***	0.12***	0.01
RVX	0.98***	0.25***	0.13**	0.07	0.86***	0.13***	0.02	-0.01
VDAX	0.97***	0.30***	0.16**	-0.11	0.87***	0.13***	0.03	0.01
VDJIA	0.95***	0.27***	0.18***	0.11*	0.82***	0.15***	0.05	0.01
VDM	0.96***	0.25***	0.19***	0.13**	0.78***	0.10**	0.09*	0.07**
VHSI	0.99***	0.20**	0.07	-0.03	0.88***	0.07*	0.01	0.05
VIX	0.95***	0.27***	0.14**	-0.06	0.77***	0.16***	0.03	0.01
VIXCAC	0.96***	0.23***	0.13**	-0.08	0.84***	0.10**	0.04	-0.01
VSTOXX	0.97***	0.25***	0.16**	0.09*	0.86***	0.12***	0.03	-0.01
VVIX	0.95***	0.25***	0.09*	-0.01	0.79***	0.14***	0.06*	-0.01
VXEM	0.98***	0.17***	0.09*	-0.07	0.86***	0.08**	-0.01	0.01
VXES	0.96***	0.28***	0.19***	-0.11	0.81***	0.14***	0.04	0.01
VXOEX	0.97***	0.20***	0.12**	0.07	0.85***	0.11**	0.05	-0.02

Table 4. Continued

Volatilities	Variance as % of observed				variance as % of the sum of all IMFs and Residue			
	HFRQ	**MFRQ**	**LFRQ**	**RESID**	**HFRQ**	**MFRQ**	**LFRQ**	**RESID**
EUVX	91.20%	5.12%	1.93%	0.01%	91.20%	5.12%	1.93%	0.01%
GVX	94.48%	7.32%	0.45%	0.01%	94.48%	7.32%	0.45%	0.01%
NVX	95.24%	2.73%	2.26%	0.01%	95.24%	2.73%	2.26%	0.01%
OVX	93.38%	7.30%	2.74%	0.03%	93.38%	7.30%	2.74%	0.03%
RVX	93.89%	3.03%	0.44%	0.01%	93.89%	3.03%	0.44%	0.01%
VDAX	90.54%	4.22%	1.01%	0.01%	90.54%	4.22%	1.01%	0.01%
VDJIA	90.49%	5.99%	1.97%	0.01%	90.49%	5.99%	1.97%	0.01%
VDM	91.76%	4.33%	1.62%	0.03%	91.76%	4.33%	1.62%	0.03%
VHSI	97.00%	1.36%	0.87%	0.01%	97.00%	1.36%	0.87%	0.01%
VIX	92.48%	6.08%	1.83%	0.01%	92.48%	6.08%	1.83%	0.01%
VIXCAC	94.61%	5.00%	0.96%	0.01%	94.61%	5.00%	0.96%	0.01%
VSTOXX	92.25%	3.08%	1.34%	0.01%	92.25%	3.08%	1.34%	0.01%
VVIX	92.94%	8.46%	0.52%	0.01%	92.94%	8.46%	0.52%	0.01%
VXEM	96.78%	3.64%	0.53%	0.01%	96.78%	3.64%	0.53%	0.01%
VXES	89.59%	4.69%	2.52%	0.01%	89.59%	4.69%	2.52%	0.01%
VXOEX	95.63%	2.93%	2.16%	0.01%	95.63%	2.93%	2.16%	0.01%

Note: HFQ, MFQ, LFQ, and RESID denote High Frequency, Medium Frequency, Low Frequency, and Residue respectively. [*], [**], and [***] indicate significance at 10%, 5% and 1% levels respectively.Table 4 presents the features of the decomposed data. The Pearson correlation coefficients and Kendall tau-b between each frequency cluster and the original/observed volatility indices. The variance proportion of each frequency cluster and the residue to the variance in the original data as well as the variance proportion of each frequency cluster to the total variance in the decomposed data. The latter should mainly corroborate with the former.

Source: own calculations based on data obtained from investing.com, R programming version 4.2.0.

Table 5. Entropy estimates of information flows between US Implied Volatility (VIX) and other volatilities – q50

	Flows towards US Implied Volatility									
	IMF1	**IMF2**	**IMF3**	**IMF4**	**IMF5**	**IMF6**	**IMF7**	**IMF8**	**IMF9**	**RS**
EUVX	-0.06	-0.10	-0.17	-0.09	-0.08	-0.07	-0.01	-0.08	-0.09	-0.15
	(0.07)	(0.08)	(0.07)	(0.06)	(0.06)	(0.07)	(0.06)	(0.08)	(0.08)	(0.04)
GVX	-0.15	-0.10	-0.09	-0.15	0.01	-0.17	-0.07	-0.06	-0.12	-0.15
	(0.05)	(0.08)	(0.07)	(0.06)	(0.06)	(0.07)	(0.07)	(0.06)	(0.08)	(0.04)
NVX	-0.11	-0.22	-0.19	-0.14	-0.09	-0.02	0.02	-0.13	-0.12	-0.16
	(0.04)	(0.08)	(0.07)	(0.06)	(0.06)	(0.07)	(0.06)	(0.08)	(0.04)	(0.04)
OVX	-0.00	0.07	0.04	-0.02	-0.09	0.01	-0.16	-0.02	-0.12	-0.08
	(0.07)	(0.08)	(0.06)	(0.07)	(0.06)	(0.06)	(0.07)	(0.07)	(0.08)	(0.08)
RVX	-0.16	-0.15	0.01	-0.01	-0.12	-0.03	-0.03	-0.12	-0.12	-0.15
	(0.07)	(0.08)	(0.06)	(0.06)	(0.08)	(0.07)	(0.06)	(0.08)	(0.08)	(0.04)
VDAX	-0.17	-0.18	-0.16	0.03	-0.11	0.15	0.00	-0.12	-0.12	-0.09
	(0.08)	(0.09)	(0.07)	(0.06)	(0.07)	(0.07)	(0.08)	(0.04)	(0.04)	(0.08)
VDJIA	0.15	-0.07	-0.20	-0.07	-0.12	-0.04	-0.02	-0.06	-0.06	-0.09
	(0.06)	(0.09)	(0.07)	(0.06)	(0.06)	(0.06)	(0.07)	(0.07)	(0.06)	(0.08)
VDM	-0.18	0.04	-0.05	-0.07	-0.02	-0.09	-0.07	-0.05	-0.06	-0.15
	(0.97)	(0.09)	(0.07)	(0.05)	(0.08)	(0.03)	(0.06)	(0.07)	(0.07)	(0.04)
VHSI	0.03	-0.11	-0.16	-0.05	-0.18	-0.05	0.02	-0.13	-0.12	-0.16
	(0.08)	(0.08)	(0.07)	(0.06)	(0.06)	(0.07)	(0.07)	(0.08)	(0.05)	(0.04)
VIXCAC	0.04	0.06	-0.07	-0.06	-0.17	-0.04	-0.01	-0.05	-0.13	-0.15
	(0.08)	(0.08)	(0.07)	(0.06)	(0.06)	(0.07)	(0.07)	(0.08)	(0.04)	(0.04)
VSTOXX	-0.16	-0.15	-0.18	0.08	0.04	-0.11	-0.02	-0.06	-0.12	-0.15
	(0.08)	(0.09)	(0.07)	(0.06)	(0.05)	(0.07)	(0.07)	(0.06)	(0.04)	(0.04)
VVIX	-0.17	-0.03	-0.11	-0.16	-0.05	-0.04	0.02	-0.12	-0.12	-0.15
	(0.07)	(0.08)	(0.07)	(0.06)	(0.07)	(0.08)	(0.08)	(0.08)	(0.08)	(0.04)
VXEM	-0.08	-0.14	-0.05	-0.16	-0.03	-0.04	0.08	0.11	-0.05	-0.09
	(0.08)	(0.08)	(0.07)	(0.06)	(0.06)	(0.08)	(0.07)	(0.07)	(0.07)	(0.08)
VXES	-0.29	-0.14	-0.19	-0.15	-0.09	-0.13	0.05	-0.05	-0.07	-0.15
	(0.07)	(0.08)	(0.07)	(0.06)	(0.06)	(0.06)	(0.07)	(0.07)	(0.07)	(0.04)
VXOEX	-0.04	-0.16	-0.18	-0.15	-0.10	-0.12	0.07	-0.03	-0.05	-0.08
	(0.06)	(0.09)	(0.08)	(0.06)	(0.07)	(0.05)	(0.07)	(0.07)	(0.07)	(0.08)

Table 5. Continued

	Flows towards other volatilities									
	IMF1	**IMF2**	**IMF3**	**IMF4**	**IMF5**	**IMF6**	**IMF7**	**IMF8**	**IMF9**	**RS**
EUVX	0.17	-0.06	-0.27	-0.14	-0.09	-0.04	-0.10	-0.07	-0.06	-0.15
	(0.07)	(0.08)	(0.07)	(0.06)	(0.05)	(0.05)	(0.07)	(0.08)	(0.08)	(0.04)
GVX	-0.19	-0.20	0.03	-0.15	-0.13	-0.04	-0.06	-0.06	-0.13	-0.15
	(0.07)	(0.09)	(0.08)	(0.06)	(0.06)	(0.06)	(0.06)	(0.08)	(0.08)	(0.04)
NVX	-0.17	-0.17	-0.13	-0.14	-0.14	-0.02	-0.01	-0.11	-0.08	-0.15
	(0.08)	(0.08)	(0.07)	(0.06)	(0.06)	(0.06)	(0.07)	(0.08)	(0.08)	(0.04)
OVX	-0.00	-0.08	-0.07	0.00	-0.08	-0.04	-0.14	-0.03	-0.12	-0.12
	(0.07)	(0.08)	(0.07)	(0.06)	(0.06)	(0.06)	(0.07)	(0.08)	(0.08)	(0.04)
RVX	-0.21	-0.16	-0.05	-0.17	-0.08	0.01	-0.02	-0.12	-0.13	-0.16
	(0.07)	(0.08)	(0.07)	(0.06)	(0.05)	(0.06)	(0.07)	(0.08)	(0.08)	(0.04)
VDAX	-0.14	-0.08	-0.15	-0.12	-0.05	-0.03	0.02	-0.08	-0.08	-0.12
	(0.08)	(0.08)	(0.07)	(0.06)	(0.05)	(0.06)	(0.06)	(0.08)	(0.08)	(0.04)
VDJIA	-0.06	-0.08	-0.15	-0.13	0.01	-0.07	0.20	-0.07	-0.07	-0.13
	(0.08)	(0.09)	(0.07)	(0.06)	(0.05)	(0.06)	(0.07)	(0.08)	(0.08)	(0.04)
VDM	-0.17	-0.08	-0.04	-0.02	0.02	0.03	-0.06	-0.05	-0.05	-0.15
	(0.07)	0.08	(0.07)	(0.06)	(0.06)	(0.06)	(0.07)	(0.08)	(0.08)	(0.04)
VHSI	-0.11	-0.23	-0.20	-0.05	0.03	0.11	0.00	-0.11	-0.08	-0.15
	(0.08)	(0.08)	(0.07)	(0.06)	(0.05)	(0.07)	(0.06)	(0.08)	(0.08)	(0.04)
VIXCAC	-0.11	-0.10	-0.05	0.03	-0.06	0.00	0.03	-0.10	-0.08	-0.15
	(0.08)	(0.09)	(0.07)	(0.06)	(0.05)	(0.05)	(0.07)	(0.09)	(0.08)	(0.05)
VSTOXX	-0.14	-0.09	-0.16	-0.14	-0.08	-0.01	0.03	-0.06	-0.09	-0.15
	(0.08)	(0.08)	(0.08)	(0.07)	(0.06)	(0.06)	(0.07)	(0.08)	(0.08)	(0.05)
VVIX	-0.14	-0.02	-0.04	0.00	-0.11	-0.11	0.00	-0.12	-0.13	-0.15
	(0.07)	(0.09)	(0.07)	(0.06)	(0.06)	(0.06)	(0.07)	(0.08)	(0.08)	(0.04)
VXEM	-0.20	-0.13	-0.12	-0.15	0.05	0.03	0.20	0.01	0.01	-0.13
	(0.07)	(0.08)	(0.07)	(0.06)	(0.07)	(0.06)	(0.07)	(0.08)	(0.08)	(0.04)
VXES	-0.23	-0.24	-0.04	-0.08	-0.09	-0.01	-0.03	-0.07	-0.05	-0.15
	(0.07)	(0.07)	(0.07)	(0.06)	(0.06)	(0.06)	(0.06)	(0.08)	(0.08)	(0.04)
VXOEX	-0.09	-0.09	-0.04	-0.08	0.01	-0.07	-0.04	-0.02	-0.04	-0.13
	(0.07)	(0.09)	(0.08)	(0.06)	(0.05)	(0.06)	(0.06)	(0.08)	(0.08)	(0.04)

Note: RETE estimates with standard errors in parenthesis.
Source: own calculations based on data obtained from investing.com, R programming version 4.2.0.

Table 6. Entropy estimates of information flows between US Implied Volatility (VIX) and other volatilities – q5

Volatility Indices	Flow Towards VIX – q5				Flow from VIX – q5			
	HFRQ	MFRQ	LFRQ	RESID	HFRQ	MFRQ	LFRQ	RESID
EUVX	0.19	-0.07	-0.01	-0.33	0.07	0.00	0.01	-0.33
	(0.14)	(0.15)	(0.13)	(0.12)	(0.13)	(0.10)	(0.12)	(0.11)
GVX	-0.00	-0.03	-0.16	-0.32	0.00	-0.27	-0.17	-0.33
	(0.15)	(0.09)	(0.12)	(0.12)	(0.16)	(0.01)	(0.13)	(0.11)
NVX	-0.11	0.30	-0.05	-0.33	-0.22	-0.10	-0.05	-0.32
	(0.14)	(0.09)	(0.12)	(0.11)	(0.14)	(0.10)	(0.12)	(0.12)
OVX	-0.01	-0.03	0.00	-0.18	-0.03	-0.12	0.00	-0.26
	(0.14)	(0.08)	(0.11)	(0.17)	(0.15)	(0.11)	(0.11)	(0.11)
RVX	0.07	0.05	-0.07	-0.32	0.08	0.00	-0.03	-0.32
	(0.14)	(0.12)	(0.11)	(0.11)	(0.14)	(0.09)	(0.10)	(0.11)
VDAX	-0.17	-0.08	-0.06	-0.20	-0.22	0.16	-0.06	-0.26
	(0.14)	(0.14)	(0.11)	(0.16)	(0.15)	(0.10)	(0.11)	(0.11)
VDJIA	-0.03	0.05	0.00	-0.19	-0.04	0.02	0.01	-0.25
	(0.15)	(0.10)	(0.12)	(0.17)	(0.14)	(0.10)	(0.12)	(0.12)
VDM	-0.00	-0.07	-0.14	-0.33	-0.12	-0.08	-0.13	-0.33
	(0.13)	(0.10)	(0.15)	(0.11)	(0.13)	(0.10)	(0.12)	(0.11)
VHSI	-0.16	-0.39	0.01	-0.32	-0.17	-0.19	-0.01	-0.32
	(0.14)	(0.13)	(0.17)	(0.11)	(0.14)	(0.10)	(0.13)	(0.12)
VIXCAC	-0.29	0.16	0.24	-0.32	-0.20	-0.00	-0.08	-0.33
	(0.15)	(0.13)	(0.12)	(0.11)	(0.15)	(0.09)	(0.13)	(0.11)
VSTOXX	-0.12	-0.28	-0.00	-0.32	-0.12	-0.28	0.06	-0.32
	(0.15)	(0.01)	(0.11)	(0.11)	(0.14)	(0.09)	(0.12)	(0.11)
VVIX	-0.01	-0.17	-0.01	-0.33	-0.09	-0.16	0.00	-0.33
	(0.15)	(0.08)	(0.17)	(0.12)	(0.15)	(0.10)	(0.11)	(0.11)
VXEM	0.07	0.19	-0.08	-0.19	-0.03	0.00	-0.08	-0.24
	(0.13)	(0.12)	(0.12)	(0.17)	(0.15)	(0.09)	(0.12)	(0.12)
VXES	-0.01	-0.19	0.25	-0.33	-0.13	0.03	-0.06	-0.33
	(0.14)	(0.11)	(0.12)	(0.11)	(0.15)	(0.11)	(0.13)	(0.11)
VXOEX	0.09	-0.19	-0.07	-0.19	-0.1	-0.05	-0.06	-0.27
	(0.15)	(0.10)	(0.12)	(0.17)	(0.14)	(0.09)	(0.12)	(0.12)

Note: RETE estimates with standard errors in parenthesis.

Source: own calculations based on data obtained from investing.com, R programming version 4.2.0.

Table 7. Entropy estimates of information flows between US Implied Volatility (VIX) and other volatilities – q 30

Volatility Indices	Flow Towards VIX – q30				Flow from VIX – q30			
	HFRQ	**MFRQ**	**HFRQ**	**MFRQ**	**HFRQ**	**MFRQ**	**HFRQ**	**MFRQ**
EUVX	0.11	-0.04	0.11	-0.04	0.11	-0.04	0.11	-0.04
	(0.06)	(0.03)	(0.06)	(0.03)	(0.06)	(0.03)	(0.06)	(0.03)
GVX	-0.00	-0.00	-0.00	-0.00	-0.00	-0.00	-0.00	-0.00
	(0.06)	(0.03)	(0.06)	(0.03)	(0.06)	(0.03)	(0.06)	(0.03)
NVX	-0.06	0.16	-0.06	0.16	-0.06	0.16	-0.06	0.16
	(0.06)	(0.03)	(0.06)	(0.03)	(0.06)	(0.03)	(0.06)	(0.03)
OVX	0.01	-0.00	0.01	-0.00	0.01	-0.00	0.01	-0.00
	(0.06)	(0.03)	(0.06)	(0.03)	(0.06)	(0.03)	(0.06)	(0.03)

Table 7. Continued

Volatility Indices	Flow Towards VIX – q30				Flow from VIX – q30			
	HFRQ	MFRQ	HFRQ	MFRQ	HFRQ	MFRQ	HFRQ	MFRQ
RVX	0.00	0.07	0.00	0.07	0.00	0.07	0.00	0.07
	(0.06)	(0.04)	(0.06)	(0.04)	(0.06)	(0.04)	(0.06)	(0.04)
VDAX	0.00	-0.06	0.00	-0.06	0.00	-0.06	0.00	-0.06
	(0.06)	(0.04)	(0.06)	(0.04)	(0.06)	(0.04)	(0.06)	(0.04)
VDJIA	-0.05	0.04	-0.05	0.04	-0.05	0.04	-0.05	0.04
	(0.06)	(0.03)	(0.06)	(0.03)	(0.06)	(0.03)	(0.06)	(0.03)
VDM	-0.025	-0.03	-0.025	-0.03	-0.025	-0.03	-0.025	-0.03
	(0.05)	(0.04)	(0.05)	(0.04)	(0.05)	(0.04)	(0.05)	(0.04)
VHSI	-0.09	-0.15	-0.09	-0.15	-0.09	-0.15	-0.09	-0.15
	(0.06)	(0.04)	(0.06)	(0.04)	(0.06)	(0.04)	(0.06)	(0.04)
VIXCAC	-0.14	0.13	-0.14	0.13	-0.14	0.13	-0.14	0.13
	(0.06)	(0.04)	(0.06)	(0.04)	(0.06)	(0.04)	(0.06)	(0.04)
VSTOXX	-0.04	-0.08	-0.04	-0.08	-0.04	-0.08	-0.04	-0.08
	(0.06)	(0.04)	(0.06)	(0.04)	(0.06)	(0.04)	(0.06)	(0.04)
VVIX	0.00	-0.06	0.00	-0.06	0.00	-0.06	0.00	-0.06
	(0.06)	(0.04)	(0.06)	(0.04)	(0.06)	(0.04)	(0.06)	(0.04)
VXEM	0.03	0.12	0.03	0.12	0.03	0.12	0.03	0.12
	(0.06)	(0.04)	(0.06)	(0.04)	(0.06)	(0.04)	(0.06)	(0.04)
VXES	0.01	-0.11	0.01	-0.11	0.01	-0.11	0.01	-0.11
	(0.06)	(0.03)	(0.06)	(0.03)	(0.06)	(0.03)	(0.06)	(0.03)
VXOEX	0.03	-0.05	0.03	-0.05	0.03	-0.05	0.03	-0.05
	(0.06)	(0.04)	(0.06)	(0.04)	(0.06)	(0.04)	(0.06)	(0.04)

Note: RETE estimates with standard errors in parenthesis.

Source: own calculations based on data obtained from investing.com, R programming version 4.2.0.

Table 8. Multi-frequency entropy estimates of information flows between US Implied Volatility (VIX) and other volatilities – at q 50

	Flows towards US Implied Volatility q -50			Flows towards other volatilities – q50		
	HFQ	MFQ	LFQ	HFQ	MFQ	LFQ
EUVX	0.14	-0.06	-0.04	0.08	0.01	0.04
	(0.09)	(0.08)	(0.07)	(0.09)	(0.06)	(0.07)
GVX	0.01	-0.01	-0.06	-0.01	-0.17	-0.08
	(0.10)	(0.06)	(0.07)	(0.10)	(0.05)	(0.07)
NVX	-0.09	0.22	-0.01	-0.17	-0.09	-0.05
	(0.09)	(0.06)	(0.07)	(0.09)	(0.06)	(0.07)
OVX	0.02	0.01	0.02	-0.01	-0.06	0.01
	(0.10)	(0.06)	(0.07)	(0.09)	(0.06)	(0.07)
RVX	0.03	0.05	-0.03	0.02	-0.04	-0.01
	(0.09)	(0.07)	(0.04)	(0.09)	(0.06)	(0.07)
VDAX	0.01	-0.08	-0.02	-0.14	0.13	-0.03
	(0.10)	(0.07)	(0.08)	(0.09)	(0.06)	(0.07)
VDJIA	-0.04	0.02	0.01	-0.05	-0.01	0.01
	(0.09)	(0.06)	(0.06)	(0.10)	(0.06)	(0.07)
VDM	-0.01	-0.04	-0.07	-0.09	-0.04	-0.05
	(0.09)	(0.06)	(0.07)	(0.08)	(0.05)	(0.07)

Table 8. Continued

	Flows towards US Implied Volatility q -50			Flows towards other volatilities – q50		
	HFQ	**MFQ**	**LFQ**	**HFQ**	**MFQ**	**LFQ**
VHSI	-0.11	-0.27	0.01	-0.10	-0.12	0.01
	(0.09)	(0.07)	(0.08)	(0.09)	(0.06)	(0.07)
VIXCAC	-0.21	0.15	0.19	-0.14	-0.05	-0.08
	(0.10)	(0.08)	(0.06)	(0.10)	(0.05)	(0.07)
VSTOXX	-0.06	-0.17	0.02	-0.07	-0.18	-0.01
	(0.11)	(0.06)	(0.08)	(0.10)	(0.06)	(0.07)
VVIX	0.01	-0.12	0.03	-0.06	-0.11	-0.01
	(0.09)	(0.06)	(0.08)	(0.10)	(0.06)	(0.07)
VXEM	0.04	0.15	-0.05	-0.04	-0.03	-0.01
	(0.09)	(0.07)	(0.07)	(0.10)	(0.07)	(0.06)
VXES	0.02	-0.17	0.19	-0.05	0.02	-0.06
	(0.10)	(0.06)	(0.07)	(0.10)	(0.06)	(0.07)
VXOEX	0.04	-0.07	-0.03	-0.02	-0.01	-0.02
	(0.09)	(0.06)	(0.07)	(0.10)	(0.06)	(0.07)

Note: RETE estimates with standard errors in parenthesis.

Source: own calculations based on data obtained from investing.com, R programming version 4.2.0.

Table 9. Multi-frequency entropy estimates of information flows between US Implied Volatility (VIX) and other volatilities – at q 80

Volatility Indices	Flow Towards VIX – 80				Flow from VIX – 80			
	HFRQ	**MFRQ**	**LFRQ**	**RESID**	**HFRQ**	**MFRQ**	**LFRQ**	**RESID**
EUVX	0.04	-0.00	-0.02	-0.02	0.02	0.04	0.08	-0.02
	(0.02)	(0.01)	(0.01)	(0.00)	(0.03)	(0.01)	(0.01)	(0.01)
GVX	0.02	-0.00	-0.01	-0.01	-0.00	-0.02	-0.01	-0.01
	(0.02)	(0.01)	(0.01)	(0.00)	(0.19)	(0.01)	(0.01)	(0.01)
NVX	-0.02	0.09	0.02	-0.02	-0.03	-0.02	-0.01	-0.01
	(0.02)	(0.01)	(0.01)	(0.00)	(0.02)	(0.01)	(0.01)	(0.01)
OVX	0.00	-0.00	0.03	-0.01	-0.00	-0.00	0.02	-0.01
	(0.02)	(0.01)	(0.01)	(0.01)	(0.02)	(0.01)	(0.01)	(0.00)
RVX	-0.01	0.05	-0.02	-0.02	-0.00	-0.01	-0.00	-0.02
	(002)	(0.12)	(0.00)	(0.00)	(0.02)	(0.01)	(0.01)	(0.00)
VDAX	0.00	-0.01	0.02	-0.01	-0.03	0.07	-0.00	-0.01
	(0.02)	(0.01)	(0.01)	(0.01)	(0.02)	(0.01)	(0.01)	(0.01)
VDJIA	-0.03	0.05	0.03	-0.01	-0.00	0.00	0.04	-0.02
	(0.02)	(0.01)	(0.01)	(0.01)	(0.02)	(0.01)	(0.01)	(0.01)
VDM	-0.01	-0.01	-0.02	-0.01	-0.00	-0.02	-0.01	-0.02
	(0.02)	(0.01)	(0.01)	(0.00)	(0.02)	(0.01)	(0.01)	(0.01)
VHSI	-0.02	-0.02	0.02	-0.01	-0.02	-0.00	-0.02	-0.01
	(0.02)	(0.01)	(0.01)	(0.01)	(0.02)	(0.01)	(0.01)	(0.00)
VIXCAC	-0.05	0.10	0.08	-0.01	-0.02	-0.02	-0.02	-0.01
	(0.02)	(0.01)	(0.01)	(0.01)	(0.02)	(0.02)	(0.01)	(0.01)
VSTOXX	0.00	-0.00	0.04	-0.01	-0.01	-0.03	0.01	-0.01
	(0.02)	(0.01)	(0.01)	(0.01)	(0.02)	(0.01)	(0.01)	(0.01)
VVIX	-0.00	-0.00	0.04	-0.02	-0.02	-0.01	0.00	-0.02
	(0.02)	(0.01)	(0.01)	(0.00)	(0.02)	(0.01)	(0.01)	(0.00)

Table 9. Continued

Volatility Indices	Flow Towards VIX – 80				Flow from VIX – 80			
	HFRQ	**MFRQ**	**LFRQ**	**RESID**	**HFRQ**	**MFRQ**	**LFRQ**	**RESID**
VXEM	0.01	0.08	-0.01	-0.01	-0.01	0.00	0.02	-0.02
	(0.02)	(0.01)	(0.01)	(0.01)	(0.02)	(0.01)	(0.01)	(0.01)
VXES	-0.01	-0.02	0.08	-0.01	-0.00	0.05	-0.02	-0.01
	(0.02)	(0.01)	(0.01)	(0.00)	(0.02)	(0.01)	(0.02)	(0.00)
VXOEX	-0.00	-0.02	-0.00	-0.01	-0.00	-0.05	-0.02	-0.01
	(0.02)	(0.01)	(0.01)	(0.01)	(0.02)	(0.01)	(0.01)	(0.00)

Note: RETE estimates with standard errors in parenthesis.

Source: own calculations based on data obtained from investing.com, R programming version 4.2.0.

Table 10. Multi-frequency entropy estimates of information flows between US Implied Volatility (VIX) and other volatilities – at q 95

Volatility Indices	Flow Towards VIX – q95				Flow from VIX – q95			
	HFRQ	**MFRQ**	**HFRQ**	**MFRQ**	**HFRQ**	**MFRQ**	**HFRQ**	**MFRQ**
EUVX	0.02	0.01	0.02	0.01	0.02	0.01	0.02	0.01
	(0.01)	(0.01)	(0.01)	(0.01)	(0.01)	(0.01)	(0.01)	(0.01)
GVX	0.02	-0.01	0.02	-0.01	0.02	-0.01	0.02	-0.01
	(0.01)	(0.01)	(0.01)	(0.01)	(0.01)	(0.01)	(0.01)	(0.01)
NVX	-0.00	0.07	-0.00	0.07	-0.00	0.07	-0.00	0.07
	(0.01)	(0.01)	(0.01)	(0.01)	(0.01)	(0.01)	(0.01)	(0.01)
OVX	0.00	-0.00	0.00	-0.00	0.00	-0.00	0.00	-0.00
	(0.01)	(0.01)	(0.01)	(0.01)	(0.01)	(0.01)	(0.01)	(0.01)
RVX	-0.01	0.07	-0.01	0.07	-0.01	0.07	-0.01	0.07
	(0.00)	(0.01)	(0.00)	(0.01)	(0.00)	(0.01)	(0.00)	(0.01)
VDAX	0.01	0.01	0.01	0.01	0.01	0.01	0.01	0.01
	(0.01)	(0.01)	(0.01)	(0.01)	(0.01)	(0.01)	(0.01)	(0.01)
VDJIA	-0.01	0.04	-0.01	0.04	-0.01	0.04	-0.01	0.04
	(0.01)	(0.03)	(0.01)	(0.03)	(0.01)	(0.03)	(0.01)	(0.03)
VDM	-0.01	-0.03	-0.01	-0.03	-0.01	-0.03	-0.01	-0.03
	(0.01)	(0.04)	(0.01)	(0.04)	(0.01)	(0.04)	(0.01)	(0.04)
VHSI	0.00	0.01	0.00	0.01	0.00	0.01	0.00	0.01
	(0.01)	(0.00)	(0.01)	(0.00)	(0.01)	(0.00)	(0.01)	(0.00)
VIXCAC	-0.01	0.09	-0.01	0.09	-0.01	0.09	-0.01	0.09
	(0.01)	(0.01)	(0.01)	(0.01)	(0.01)	(0.01)	(0.01)	(0.01)
VSTOXX	0.02	0.02	0.02	0.02	0.02	0.02	0.02	0.02
	(0.01)	(0.01)	(0.01)	(0.01)	(0.01)	(0.01)	(0.01)	(0.01)
VVIX	-0.00	0.02	-0.00	0.02	-0.00	0.02	-0.00	0.02
	(0.01)	(0.01)	(0.01)	(0.01)	(0.01)	(0.01)	(0.01)	(0.01)
VXEM	0.01	0.06	0.01	0.06	0.01	0.06	0.01	0.06
	(0.01)	(0.01)	(0.01)	(0.01)	(0.01)	(0.01)	(0.01)	(0.01)
VXES	0.01	0.04	0.01	0.04	0.01	0.04	0.01	0.04
	(0.01)	(0.01)	(0.01)	(0.01)	(0.01)	(0.01)	(0.01)	(0.01)
VXOEX	-0.00	-0.01	-0.00	-0.01	-0.00	-0.01	-0.00	-0.01
	(0.01)	(0.01)	(0.01)	(0.01)	(0.01)	(0.01)	(0.01)	(0.01)

Source: own calculations based on data obtained from investing.com, R programming version 4.2.0.

Figure 1. Plots of price and returns series

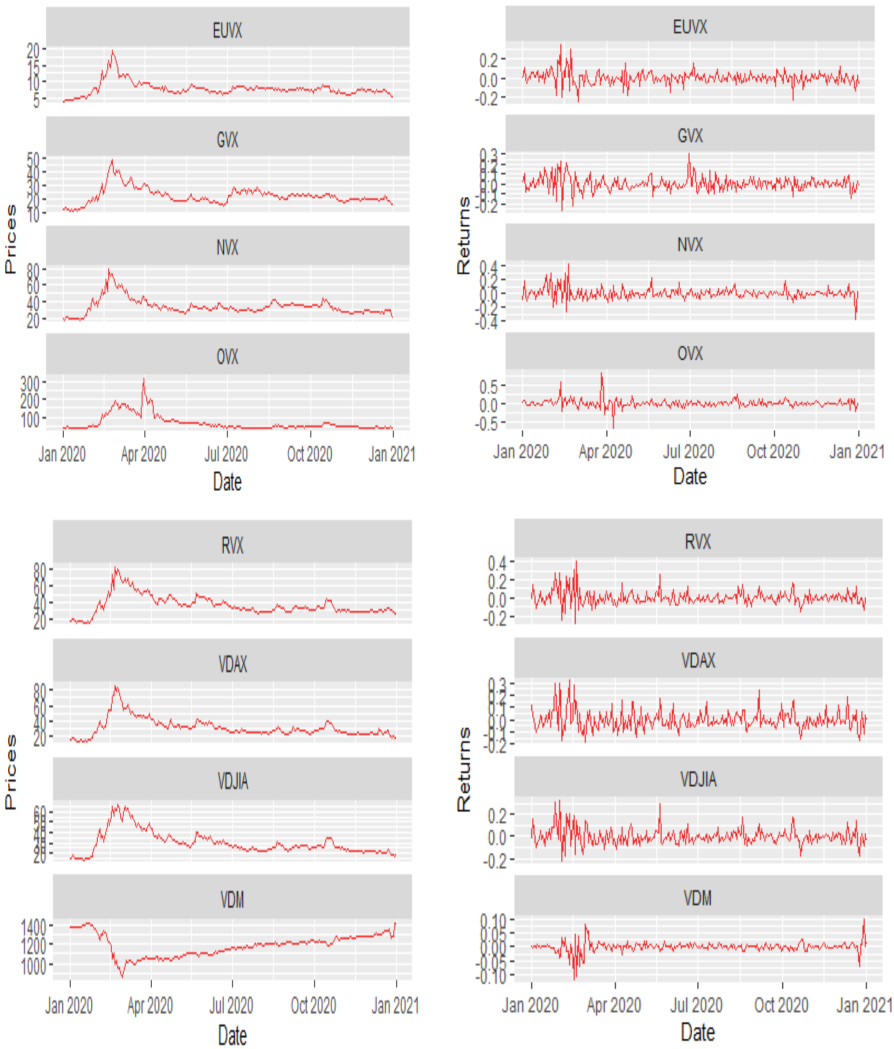

Figure 1. Continued

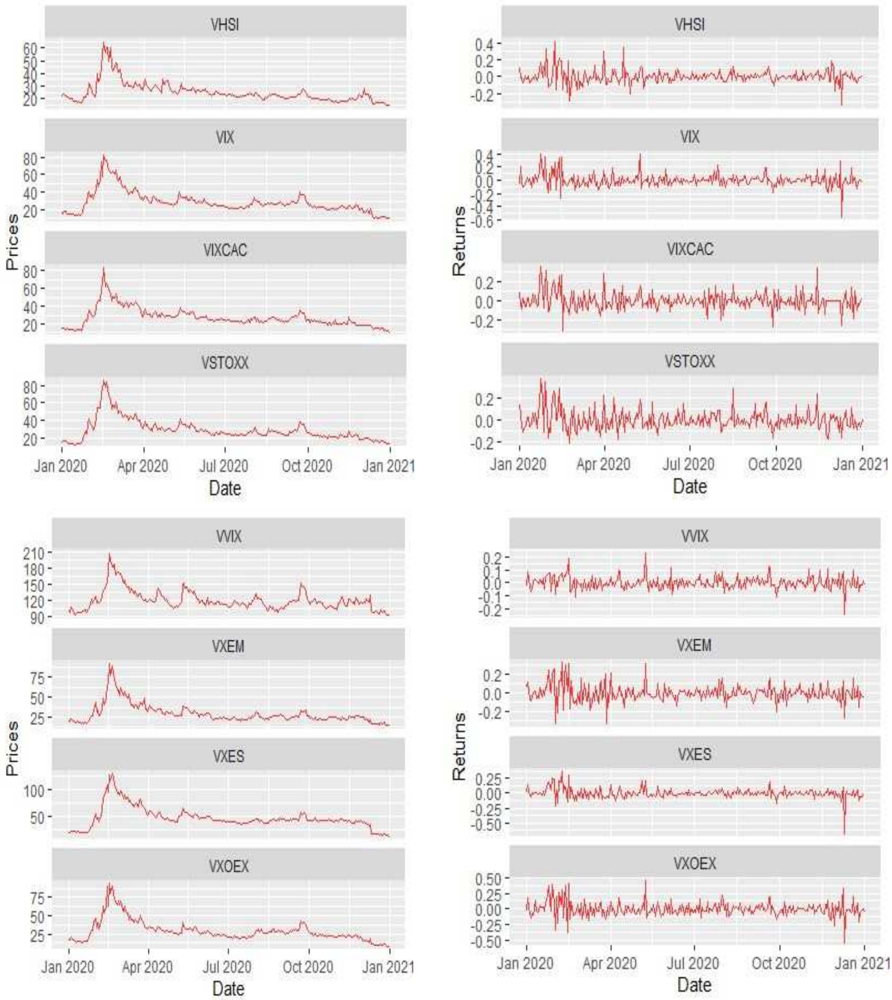

Source: own calculations based on data obtained from investing.com, R programming version 4.2.0.

Figure 2. Multi-frequency information flows between VIX and other volatilities returns – q50

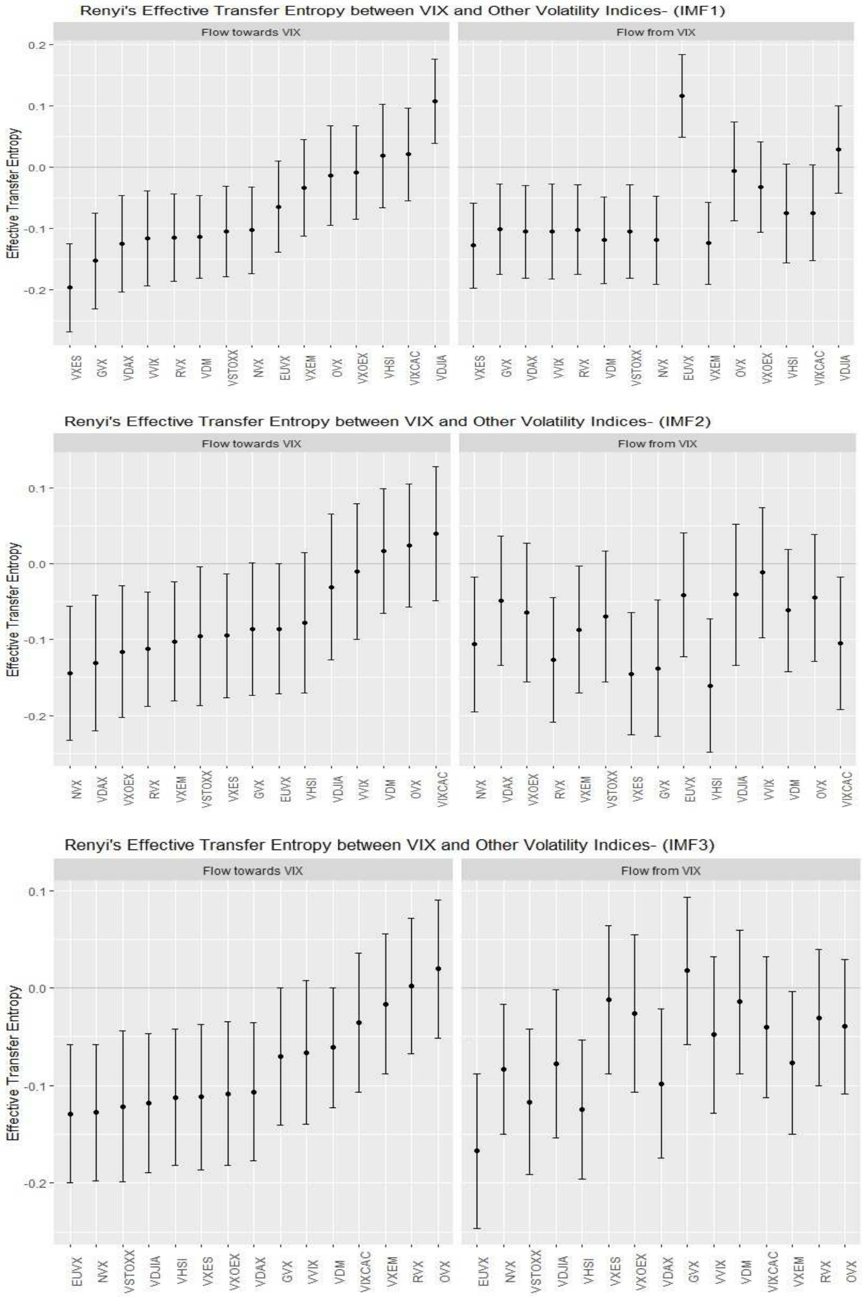

Figure 2. Continued

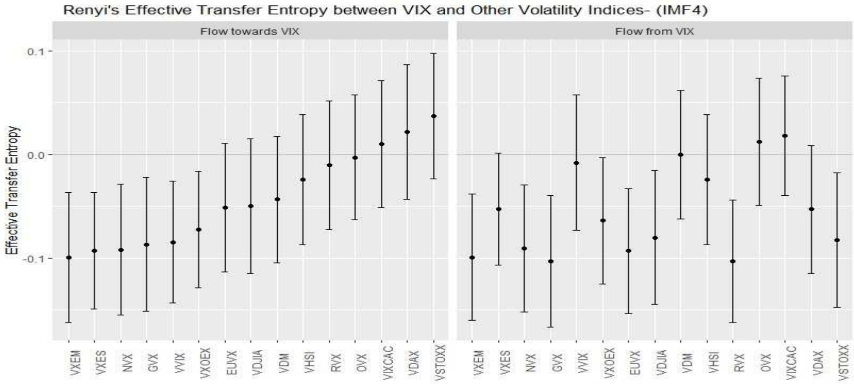

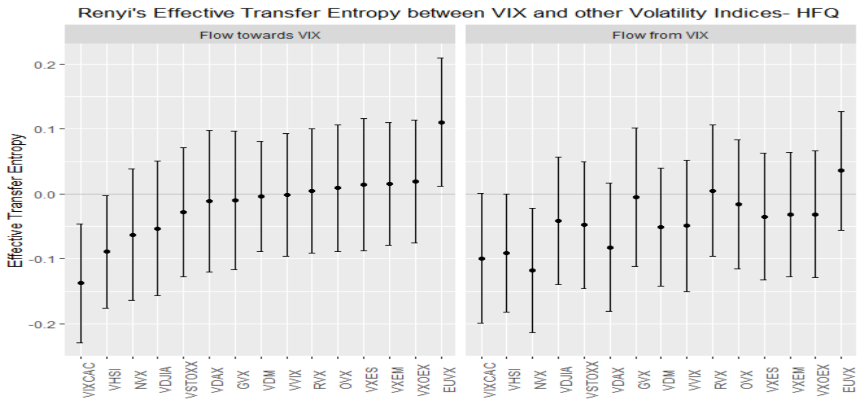

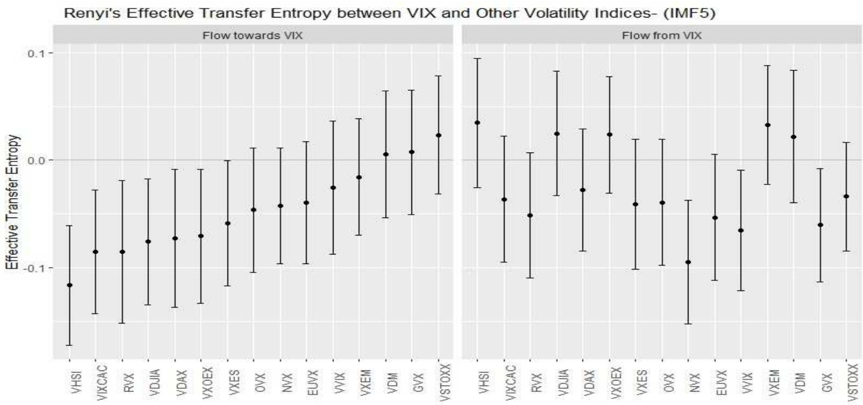

Figure 2. Continued

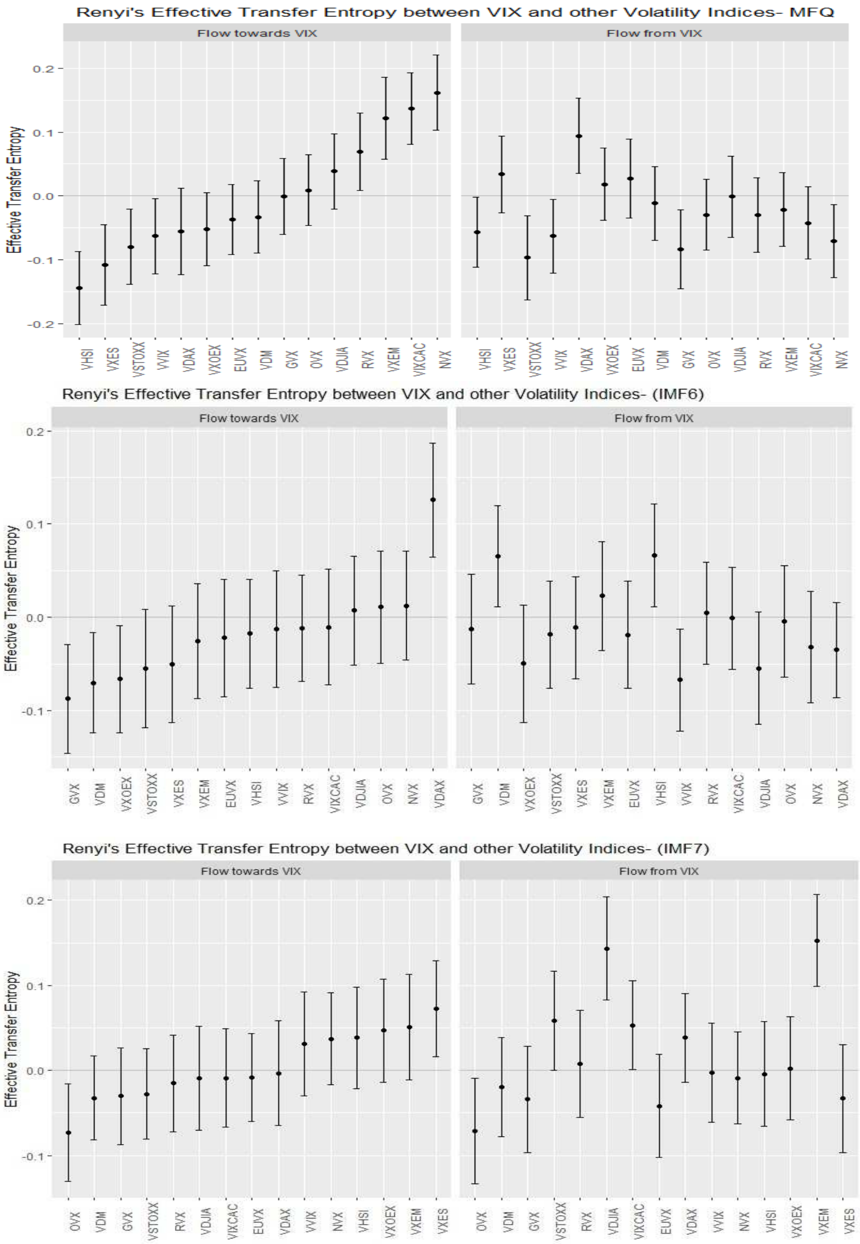

Figure 2. Continued

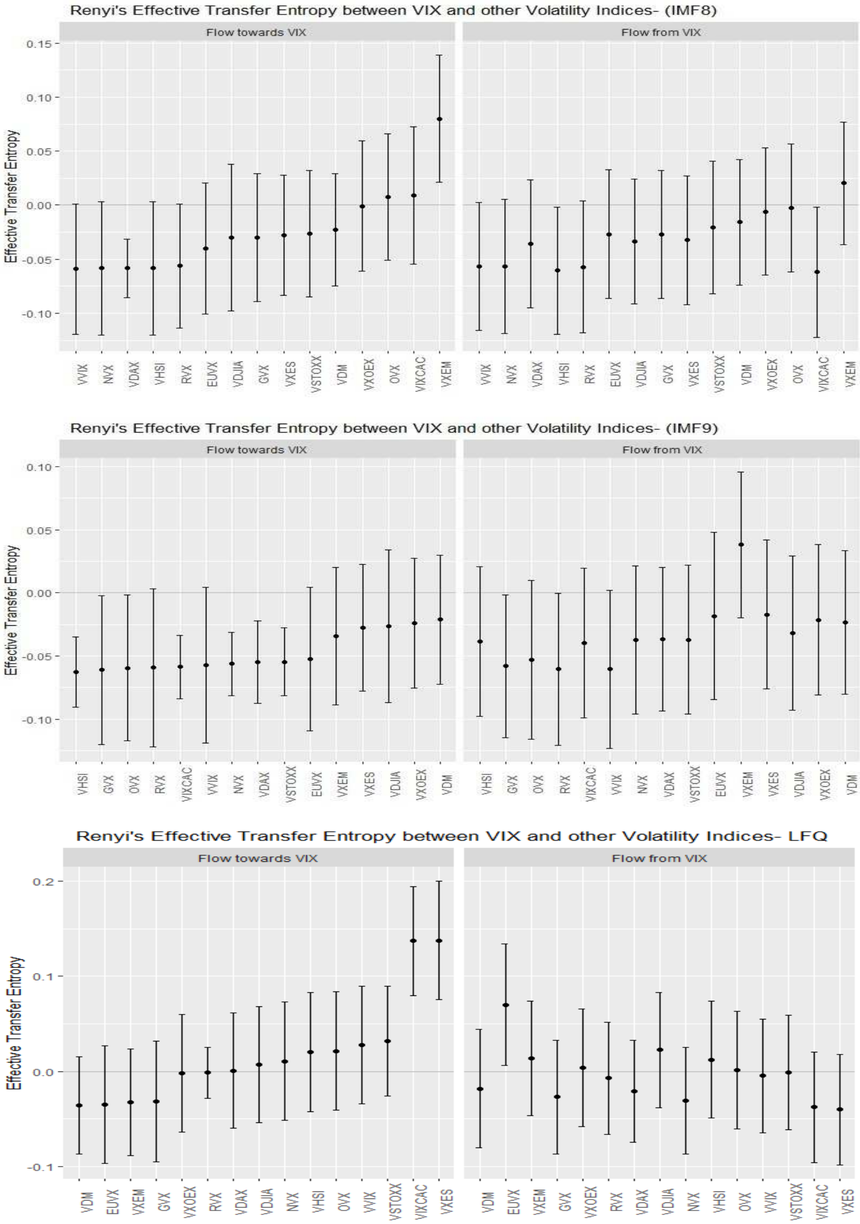

Figure 2. Continued

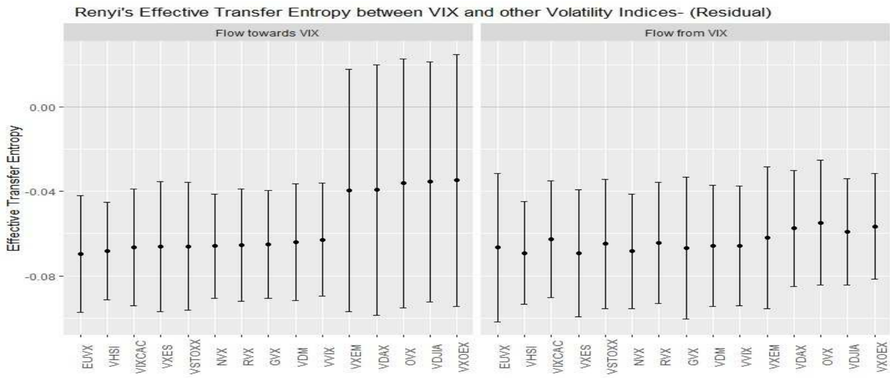

Source: own calculations based on data obtained from investing.com, R programming version 4.2.0.

Figure 3. Multi-frequency information flows between VIX and other volatilities returns – q5, 30, 80, and 95

q-5

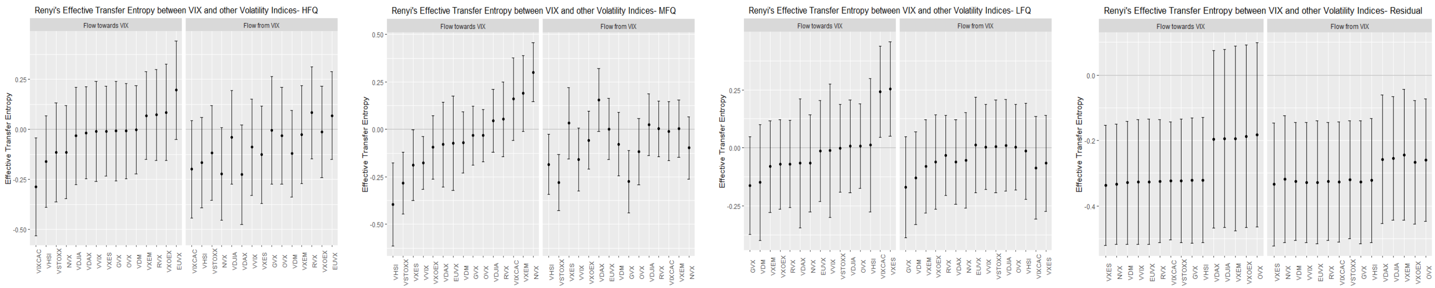

q-30

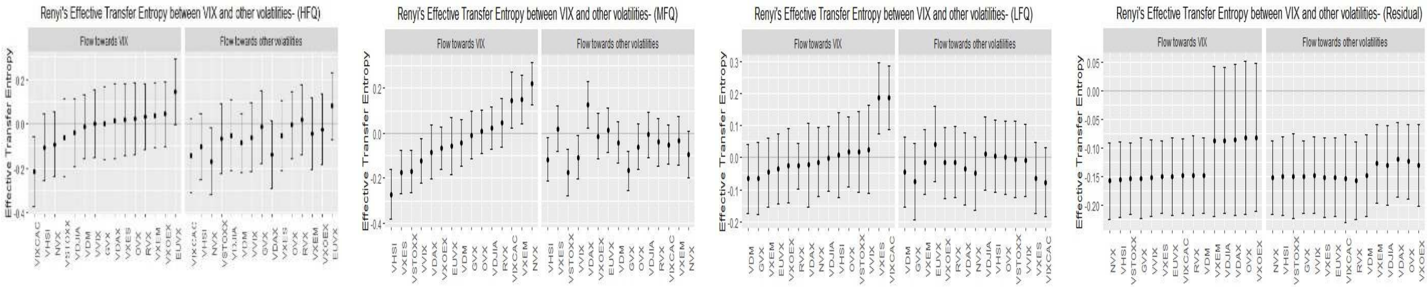

Figure 3. Continued

q-80

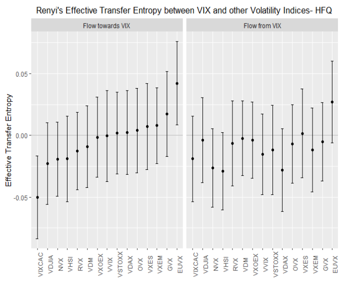

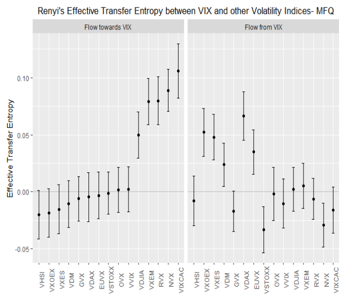

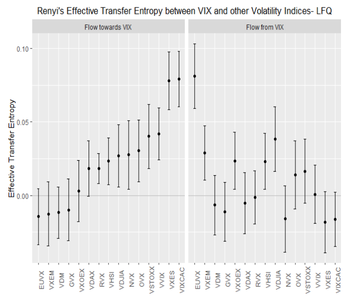

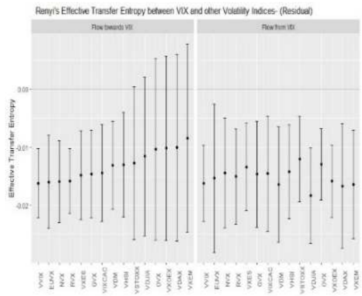

q-95

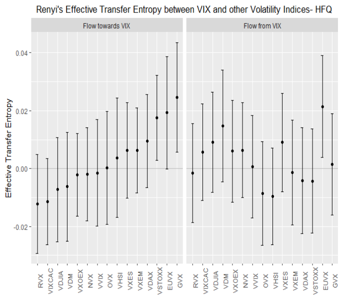

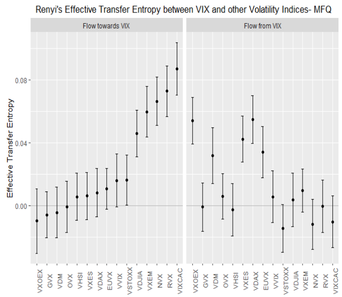

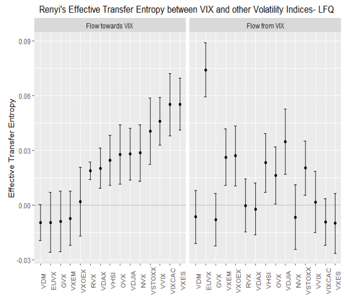

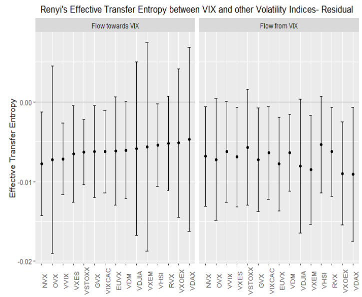

Source: own calculations based on data obtained from investing.com, R programming version 4.2.0.